

ADOSP-03-72-1005

von **KARMAN INSTITUTE**  
FOR FLUID DYNAMICS

AD 740989

FINAL SCIENTIFIC REPORT

LOW DENSITY HIGH TEMPERATURE GAS DYNAMICS

70 May 01 - 71 October 31

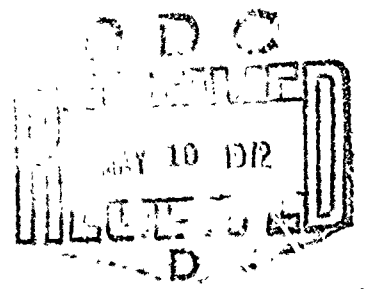
by

J.J. SMOLDEREN

and

J.F. WENDT

Reproduced by  
**NATIONAL TECHNICAL  
INFORMATION SERVICE**  
Springfield, Va. 22151



RHODE-SAINT-GENESE, BELGIUM

1972 JANUARY '31

72 January 31

FINAL SCIENTIFIC REPORT

LOW DENSITY HIGH TEMPERATURE GAS DYNAMICS

70 May 01 - 71 October 31

J. J. SMOLDEREN

and

J. F. WENDT

von Karman Institute for Fluid Dynamics  
Rhode-Saint-Genèse, Belgium

~~THIS DOCUMENT HAS BEEN APPROVED FOR PUBLIC  
RELEASE AND IS IN THE PUBLIC DOMAIN~~

This research has been sponsored in part by the Air Force  
Office of Scientific Research through the European Office  
of Aerospace Research (OAR), United States Air Force under  
Grant EOOAR 70-0081.

### ACKNOWLEDGEMENTS

The authors gratefully acknowledge the major contributions to this study by Mr. Fernand De Geyter, Research Assistant in the Low Density Laboratory. He will present the work reported herein to the University of Leuven in partial fulfilment of the requirements for a Ph.D. degree. Mr. De Geyter's activities were partially supported by the I.W.O.N.L., Belgium. A preliminary report on this work was presented by Mr. De Geyter at the I.A.F. Student Conference of the 22nd I.A.F. Congress in Brussels during September 1971.

Acknowledgement is also accorded to Mr. Michael Reynolds, Research Assistant, for his suggestions on aspects of the experimental design and for his aid in carrying out the tests.

# ABSTRACT

An experimental study was performed to determine the nature of the disturbance to the free stream density in the vicinity of the leading edge of a wedge. A number of wedge angles and leading edge thicknesses were chosen so as to examine the effect of geometry. The development of a modulation technique, wherein a two-dimensional wedge was transformed into a spinning four-sector disc, allowed the quantity  $\Delta\rho = \rho(x,y) - \rho_\infty$  to be measured directly with an accuracy comparable to that normally attained in a measurement of  $\rho$ . The experiments were performed in a free jet flow field.

The principal conclusions of this study are :

1. The appropriate scaling length for upstream disturbances is  $\lambda_{bf}$ , the body-free stream mean-free-path.

2. A negligible influence of leading edge bluntness on upstream density requires that the leading edge thickness obey the relationship :

$$\tau_{L.E.} \leq \lambda_{bf}/S_\infty.$$

3. Upstream influence is strongly affected by both  $\tau_{L.E.}$  and  $\omega$ , the wedge total angle.

4. Limiting on-axis values for  $\Delta\rho/\rho$  corresponding to the infinitely-thin flat plate case ( $\omega \rightarrow 0$ ,  $\tau_{L.E.} \rightarrow 0$ ) have been determined by extrapolation for various values of  $x/\lambda_{bf}$  upstream. At  $x \approx .1 \lambda_{bf}$ ,  $(\Delta\rho/\rho)_{\text{flat plate}}$  is  $\sim 5\%$ .

5. When the disturbance region is scaled by  $\lambda_{bf}$  over a distance downstream of the leading edge equal to  $\sim 1 \lambda_{bf}$ , experimental data which cover the range  $6 < M_\infty < 26$  and  $0.25 < T_b/T_0 < 1.0$  show good agreement. In addition, Monte Carlo results for  $M_\infty = 13$ ,  $T_b/T_0 = 0.1$  exhibit equally good agreement.

TABLE OF CONTENTS

	page
ACKNOWLEDGEMENTS .....	i
ABSTRACT .....	ii
NOMENCLATURE .....	iv
INTRODUCTION .....	1
DESCRIPTION OF EXPERIMENTAL ARRANGEMENT .....	4
A. Principle of Modulation Technique .....	4
B. Experimental Setup .....	6
C. Electron Beam Probe and Associated Electronics ...	6
D. Models .....	7
E. Flow Field .....	8
F. Calibration .....	10
EXPERIMENTAL PROGRAM .....	12
A. Test Procedure .....	12
B. Results .....	13
C. Comparisons with other Results .....	18
CONCLUSIONS .....	22
REFERENCES .....	25
TABLE 1 .....	28
FIGURES .....	31

## NOMENCLATURE

### Symbols

c	Average thermal velocity
D	Effective diameter of free-jet orifice
I	Intensity
M	Mach number
n	Number density
p	Pressure
S	Speed ratio $= \frac{u}{\sqrt{2RT}} = \sqrt{\frac{\gamma}{2}} M$
$V_{rel}$	Relative velocity between a free stream molecule and a molecule emitted by the body.
x	Length coordinate parallel to free stream velocity
y	Length coordinate perpendicular to free stream velocity
$\lambda$	Mean free path
$\rho$	Mass density
$\Delta\rho$	$\rho - \rho_\infty$
$\sigma$	Collision cross section
$\tau$	Thickness
$\omega$	Total wedge angle

Subscripts

L.E.	Leading edge
"	Free stream conditions
b	Body (model) conditions
bf	Collision between a "body" molecule and a cloud of free-stream molecules
0	Stagnation conditions
fb	Collision between a free-stream molecule and a cloud of "body" molecules

## INTRODUCTION

The hypersonic flow over a flat plate with sharp leading edge has been studied extensively during the past ten years. The interest in this problem results from the fact that a proper description of such a flow field in what have now been termed the "kinetic" and "transitional" regimes (possibly also the early stages of the "merged-layer" regime) cannot be provided by the Navier-Stokes equations of continuum gas dynamics. Experimental evidence and the results of certain approximate theoretical treatments (see, e.g., Refs. 1-17) have therefore been employed to construct a variety of flow models for these non-continuum regimes.

Whereas theoretical studies of the problem have always dealt with infinitely thin flat plates, it has long been realized that in an experimental situation the shape of the leading edge may have a marked influence on the development of the flow above the plate. The criteria employed in many early studies which concentrated on the strong and weak interaction regions can be summarized as follows:

If the wedge angle is smaller than the Mach angle and if the wedge is "aerodynamically" sharp (i.e. thickness of wedge not large compared to a free-stream mean-free-path), then the influence of the edge geometry can be neglected.

Considerable evidence exists to support the view that such criteria are not adequate when attention is focused on the regions forward of and including the merged-layer regime. This is easily visualized when one considers that the molecular flux to the plane of the leading edge is of order  $S_\infty$  times larger than the flux to the plane of the plate in the vicinity of the leading edge. In addition, if one focuses attention on the region upstream of and near to the plane of the leading edge, it is seen from angular considerations that virtually all reflected molecules found in this region come from the leading edge and not the upper plate surface. Finally, the lower surface



of all "flat" plates with finite bevel angle will always contribute more strongly to the flow disturbance immediately upstream of the leading edge than will the upper surface.

Thus, it is clear that leading edge geometry; i.e., thickness and bevel angle; must affect the flow upstream of the leading edge and therefore must influence the initial stages of flow field development along the plate.

Previous studies which have contributed specific information regarding the effect of geometry on the upstream influence (or on the downstream region a few mean-free-paths from the leading edge) are briefly summarized in the following paragraphs.

Becker and Boylan (Ref. 1) investigated the effect of wedge angle and leading edge thickness with the aid of impact probe surveys downstream of the leading edge of a flat plate in a hypersonic flow.

Hickman (Ref. 2) has made density surveys with an electron beam probe upstream and downstream of the leading edge of two flat plates with markedly different geometries. In addition, he has also surveyed the flow on the wedge-side of the same flat plate (Ref. 3).

Joss and Bogdonoff in two separate papers (Refs. 4, 5) have presented experimental data obtained with an electron beam probe, radiating hot wires, and surface pressure taps, in the vicinity of the leading edge of a sharp flat plate. The effect of leading edge thickness was investigated.

Vidal, Merritt, and Bartz (Ref. 6) have presented surveys with a speed-ratio probe upstream and downstream of three different leading-edge configurations.

To our knowledge, no theoretical studies have been performed to study the effect of edge geometry on flow field disturbances. However, as Vogenitz, Broadwell, and Bird (Ref. 7) point out in their Monte-Carlo treatment of the infinitely thin flat plate, "A few flow features (of the Monte Carlo results) are not in agreement with the (experimental) data, and it may be that the data are influenced by factors not represented in the

theory. In particular, leading edge thicknesses small compared to  $\lambda_\infty$  and small lower surface angles may still have important effects on high Mach number leading edge flows". (Notes in parentheses are ours).

The previously-cited experimental studies, in our opinion, have not provided sufficiently precise flow-field information under suitable conditions to permit a systematic study of the effect of leading edge geometry on flow-field development in the vicinity of the leading edge. The objective of the present research work is thus to provide further experimental data on the density disturbance ahead of the leading edge and in the early stages of the kinetic region. To be considered useful, the results are required to have sufficient precision and to represent properly selected conditions such that a systematic analysis of the effect of leading edge geometry on flow field development can be achieved.

In brief, a mapping of the flow density around the model was performed with an electron beam fluorescence probe (Ref. 18). A "modulation" technique was developed to improve the accuracy of relative density measurements determined with such an instrument. The objective of this technique is to obtain directly the quantity of interest, namely  $\Delta\rho(x,y) \equiv \rho(x,y) - \rho_\infty$  with an accuracy comparable to the steady state measurement of  $\rho(x,y)$ . The hypersonic low-density flow was produced by a free-jet expansion. The models were wedges symmetric with respect to the flow axis. A wedge was chosen rather than an asymmetric flat plate because it was felt that a symmetric arrangement was more appropriate for a systematic study. The effect of different total wedge angles ( $\omega$ ) and leading edge thicknesses ( $r_{L.E.}$ ) on  $\Delta\rho$  was studied. By extrapolating the results to the case  $\omega \rightarrow 0$  and  $r_{L.E.} \rightarrow 0$ , the conditions which apply to an infinitely thin flat plate can then be realized.

The following sections describe the principle of the modulation technique and its operation in practice, the results of density measurements in the vicinity of the leading edge region for a variety of wedges in a hypersonic flow, and the conclusions drawn from these results.

## DESCRIPTION OF EXPERIMENTAL ARRANGEMENT

### A. Principle of Modulation Technique

The basic quantity of interest at any point  $(x, y)$  in the flow field relative to the model is :

$$\frac{\Delta \rho(x, y)}{\rho} = \frac{\rho(x, y) - \rho_{\infty}}{\rho_{\infty}}$$

which, in words, may be expressed as :

$$\frac{\rho_{\text{disturbed}} - \rho_{\text{freestream}}}{\rho_{\text{freestream}}} \quad \text{or} \quad \frac{\rho_{\text{with model}} - \rho_{\text{without model}}}{\rho_{\text{without model}}}$$

With the classical method, employed in all earlier experimental work, this quantity has been obtained by performing two steady state measurements with an electron beam probe yielding  $\rho_{\text{disturbed}}$  and  $\rho_{\text{freestream}}$  separately. Because of instabilities and noise problems inherent in the operation of an electron-beam probe, such measurements have a limited accuracy. In regions where  $\rho_{\text{disturbed}}$  and  $\rho_{\text{freestream}}$  differ only slightly from one another, the relative error in  $\Delta \rho$  becomes so large as to prevent the observation of any detailed flow variations. For the present study a new measurement technique has been developed to overcome this basic limitation. The objectives of this method are two-fold :

- to bring out directly the magnitude of the disturbance,  $\Delta \rho$ , with an accuracy comparable to that achieved when measuring  $\rho_{\infty}$  ;
- to obtain  $\Delta \rho$  and  $\rho_{\infty}$  simultaneously.

The principle underlying the technique is as follows : if the model can be brought in and out of the flow periodically, the density probe will measure, during one half-period,  $\rho_{\text{with model}}$  ; during the next half-period,  $\rho_{\text{without model}}$  (i.e.,  $\rho_{\infty}$ ). The amplitude of the square wave variation is thus directly proportional to the desired quantity,  $\Delta \rho$ . Taking advantage of synchronous

detection techniques (lock-in amplification), the accuracy of the difference measurement becomes comparable to the accuracy of an absolute one. In essence, one repeats two absolute measurements a great many times and takes the average of the difference over a long period. The D.C. component of the signal can be measured simultaneously with the amplitude of the modulation. From these two pieces of information, the ratio  $\Delta\rho/\rho$  can be immediately computed. The procedure is outlined schematically in Fig. 1. Another advantage of this method is that the result is insensitive to changes in the response of the density probe because they would act simultaneously on the quantities B and C defined in the figure. Thus, the influence of changes (or drift) in beam current, beam focusing, sensitivity of photomultiplier tube and optics, etc., is drastically reduced.

The use of a lock-in amplifier to measure the amplitude of the signal sets a lower limit to the frequency with which the model can be displaced since the instrument's performance improves with increasing frequency. Mechanical considerations will set an upper limit. The inertia of any model of reasonable size excludes a linear square-wave type displacement. To overcome this problem, a large-diameter four-sector disc (Fig. 2) replaces the conventional two-dimensional wedge. With the disc spinning in the flow, the desired modulation effect is achieved, providing the difference between the disc's outer radius and hub radius is very small compared with a mean-free-path. If the extent of the region of interest in the vicinity of the leading edge is small compared to the disc radius, the disc then approximates a wedge of infinite extent.

It should be noted that the effect of the transition time (when the edge of each wedge sector passes the measurement point) is not proportional to the ratio of transition time to rotation period (as one might expect at first glance), but rather to the square of this quantity and thus the transition effect can safely be neglected. This is due to the manner in which the lock-in amplifier treats the signal - it is essentially multiplied by a sine-wave in phase with the angular rotation of

the disc. Thus, just at the transition point, the signal is multiplied by a very small factor (sine-wave value close to zero).

#### D. Experimental Setup

The experiment was arranged in the V.K.I. Low Density Wind Tunnel (Ref. 19). A photograph of the installation is shown in Fig. 3. Each wedge-shaped disc model was mounted on a shaft which in turn was geared to the axis of a heavy-duty synchronous motor. The rotation rate of the models was chosen to be 15 Hz; thus, the modulation frequency was 30 Hz (two "leading edges" per disc). The model axis can be varied with respect to the flow axis so that for example the flow around a flat plate with bevel angle  $\alpha$  may be studied with the same model previously used as a wedge of total angle  $\alpha$ . A signal proportional to the rotational frequency, used as the reference frequency for the lock-in amplifier, is provided by a resolver fixed to the model shaft.

#### C. Electron Beam Probe and Associated Electronics

The fluorescence of an electron-beam is employed to measure density. The beam is created by an oxide-coated TV-type gun located in a gun chamber separated from the tunnel ambient pressure by a two-stage differential pumping system. The optical detector consists of a lens-slit-flexible light guide - photomultiplier assembly (Fig. 4). The gun chamber and optics are mounted on a three-dimensional traversing mechanism located at the base of the tunnel. The accuracy of the short-range positioning system is better than 0.1 mm. The photomultiplier is fixed on the outside of a window in the wall of the tunnel and is kept at room temperature.

As the significant gradients in density occur in the axial flow direction and as the beam has an unknown intensity distribution over its nearly circular cross-section, an "effective" beam diameter has to be determined to delineate the volume to

which the measured density corresponds. This was done by using the spinning disc as a knife edge as shown in Fig. 5. The electron current collected by the Faraday cup was recorded as the beam was moved axially across the disc-edge. The profile is seen to be symmetric and quite linear in the central region. This indicates that the current density over the majority of the beam cross-section is nearly constant. The test also demonstrates that the impingement of the electron beam on the sharp edge of a metal surface does not result in a noticeable deflection of the beam, at least up to the point of beam impact.

The electron beam was operated during most of the tests reported herein at 17 kV and 200  $\mu$ amps cup current. Typically, the cup current can be held constant to within  $\pm 3\%$  by manually adjusting the grid potential. However, as noted earlier, such a variation is not important since absolute intensity (i.e.,  $\rho_\omega$ ) is measured simultaneously with the fluctuating component (i.e.,  $\Delta\rho$ ).

The system which senses the intensity of fluorescence is shown schematically in Fig. 2 where the essential components are :

- photomultiplier (EMI 9502 S)
- electrometer (KEITHLY 610 B) for measuring the D.C. component of the signal
- low noise pre-amplifier plus filter (PAR CR-4) for blocking the D.C. component and reducing excessive A.C. noise at frequencies other than 30 Hz
- lock-in amplifier (PAR JB-5) whose read-out is proportional to the amplitude of the A.C. component of the signal.

#### D. Models

Four-sector discs having a diameter of 30 cm serve as the models. Because the extent of the test region is small with respect to the curvature of the edge, the model approximates an infinitely long wedge with straight leading edge. The portion of the disc which has a wedge-shaped cross-section extends for at

least 5 cm behind the leading edge. It can be easily appreciated that high precision is required in machining each disc. Over the complete circumference, the maximum variation in leading edge thickness is 0.02 mm, the maximum variation in wedge angle is  $0.2^\circ$ , and the maximum variation in disc radius is 0.05 mm. The models were aligned by running a needle, with its point on the axis of the flow, along the cut in the disc at the edge of a sector starting from the center of the leading edge. Mis-alignment with the flow axis was held to well under  $0.5^\circ$  by this technique. No asymmetry in density profiles at a fixed upstream position was ever detected within the limits of data scatter; thus, the alignment technique was sufficiently precise for the present study.

The discs are coated with graphite to reduce both optical reflection and the emission of secondary electrons resulting from the impingement of the beam on the disc surface when the region downstream of the leading edge is under investigation.

A number of different models were employed spanning the following ranges for the two variable geometrical parameters (see also Table 1) :

Leading edge thickness :  $0.05 \text{ mm} \leq r_{L.E.} \leq 0.5 \text{ mm}$

Wedge total angle :  $6^\circ \leq \omega \leq 20^\circ$

#### E. Flow Field

The flow field employed for these studies was a free jet expansion (Ref. 20). Using the electron beam fluorescence probe, a number of experiments were performed to determine the useable region of the expansion. Since all axial flow-field parameters are conditioned by the stagnation pressure ( $p_0$ ) and the position in the free-jet ( $x/D$ ), their useful range is determined by requiring that :

- the upstream influence of the Mach-disc should produce no more than a 2% deviation between the experimentally measured density and the theoretical inviscid value at the measurement station

- the correction to flow field parameters due to viscous effects, freezing, and condensation should be small because of the inability to predict them accurately. Condensation effects are indeed negligible using criteria advanced in Ref. 21. Furthermore, the other effects are of secondary importance for the present problem. The density disturbance field is strongly conditioned by collisions between molecules reflected from the surfaces of the wedge and incoming molecules. The scattering characteristics of this collision process are primarily a function of the velocity and direction of the two classes of molecules. For the molecules leaving the body these quantities are determined by the wall temperature and orientation; while incoming molecules are all close to terminal velocity in any case, if the flow is hypersonic. In any event, the correction to the Mach number as given by Ref. 22 was kept less than 5% for all conditions of  $p_0$  and  $x/D$  considered. It is possible that moderate rotational freezing (Ref. 23, 24) occurred upstream of the measurement point in some cases, but always downstream of the point where the flow was already hypersonic.

In summary, the ranges of the relevant inviscid theoretical flow parameters in the experiments reported herein are :

- Gas : air
- Stagnation temperature : room temperature ( $\sim 300^\circ\text{K}$ )
- Mach number : 6 - 11 (Speed ratio : 5 - 9 )
- Free-stream mean-free-path : 0.5 mm - 3.0 mm
- Orifice diameter : 5 mm.

A complete list of flow-field properties for the different runs is given in Table 1. The test region extended from 1 cm upstream to 0.5 cm downstream of the leading edge. The magnitude of the axial variation in free-stream flow properties over this region is also given in Table 1.



## F. Calibration

The proportionality factor  $K$  between the output of the lock-in amplifier and the amplitude of the density disturbance ( $\Delta\rho$ ) must be determined by a suitable calibration. Two methods were employed :

1. Using a function generator with a variable D.C. bias, a square-wave signal of known amplitude was fed into the electrometer. The amplitude of the square wave and the average value of the signal were changed independently and the electrometer and lock-in outputs were recorded. The results, normalized by the average value, are plotted as closed circles in Fig. 6.
2. In the process of making an experimental run, the periodic change in the signal, for points close to the leading edge, is strong enough to be measured with an oscilloscope connected between the output of the electrometer and the input to the preamplifier. The results, normalized by the average value of method 1, are shown as open circles.

Comparing the results from these two calibration methods, the following conclusions can be drawn :

1. The proportionality factor is constant over the entire range of  $\Delta\rho/\rho$ .
2. Although the signal on the oscilloscope in the second method is noisy, the R.M.S. deviation in the value of  $K$  is less than 2%.
3. The average value of  $K$  determined by each method is virtually the same. Since method 2 employs the spinning disc and method 1 does not, this result indicates that the disturbance is not distorted by the use of a sector disc and that transition effects associated with the edge of each sector are indeed negligible.

Method 2, which provides a direct calibration in a true experimental situation, was used systematically in the experiments and provided a check on the stability of the system. A third method was used occasionally : the beam may be chopped completely when moved downstream of the leading edge. By focusing

on a point above the wedge (the beam emanates from below), the resulting signal is such that the amplitude of the modulation must be equal to twice the D.C. component. The results of this test correspond to a single point on Fig. 6 (with total spread indicated). Thus the ratio of the lock-in output to the electrometer output under this condition provides a simple check on the calibration constant.

## EXPERIMENTAL PROGRAM

### A. Test Procedure

A number of preliminary experiments were performed to determine the regions in the flow where no spurious effects occurred due to the particular experimental arrangement.

1. As stated earlier, the free-jet was probed in the absence of the model and thus the useable test region in the axial direction was delineated according to the criteria mentioned in the section entitled "Flow Field". It was also verified that the density varied radially by no more than 2% over the extent of the test region.
2. The minimum detectable upstream influence from the shaft and hub region of the disc was found experimentally to be far downstream (i.e., many tens of mean-free-paths) from the test region.
3. A measurement of the fluorescence very close to the model surface with no flow (but with the model spinning to enable very small signals to be recorded) may indicate a finite  $\Delta\rho$  when no signal should be observed at all. This result is clearly due to the combined effect of optical reflection and beam impingement on the model (for regions behind the leading edge). The extent of the test region was therefore always limited to that portion wherein the error in  $\Delta\rho/\rho$  so introduced was less than 5%.

The final data were recorded by performing a large number of radial scannings at different axial distances from the leading edge for each model. By cross-plotting the results a map of the density disturbance over the entire test region may be constructed. The density disturbance,  $\Delta\rho(x,y)$  is normalized in each case by the local free stream density,  $\rho_\infty(x,y)$ . For a given model, different maps were produced by varying the stagnation pressure so as to change  $\lambda_\infty$ , and by varying the leading edge position so as to change Mach number. Although the Mach number was varied from 6 to 11, most of the data presented are for

$M_\infty = 9$ . No Mach-number effect was evident in the tests reported herein.

## B. Results

An example of a typical set of data is shown in Fig. 7. Each data point is the unreduced output of the lock-in amplifier. The radial profile extending equally far on both sides of the axis indicates that the disturbance,  $\Delta p$ , is indeed symmetric. Full radial profiles were recorded for each model as a check on alignment. It should be noted that the scatter in the results is reasonably low even for the smallest value of the disturbance. The profiles all exhibit a single maximum on the axis, even for the case of the wedge with the smallest total angle ( $6^\circ$ ) and leading edge thickness (0.05 mm).

Figs. 8 and 9 present two examples of a two-dimensional disturbance map. The flow conditions are indicated. In Fig. 8, the case for the smaller mean-free-path, initial stages of the formation of a shock wave downstream from the leading edge are clearly seen. Note also that the region of maximum gradient occurs in a plane passing through or slightly behind the leading edge. The disturbance to the free stream density is seen to exist many mean-free-paths upstream of the leading edge.

The on-axis upstream influence produced by four  $10^\circ$  wedges with distinctly different values of leading edge thickness (ranging from 0.05 mm to 0.90 mm) is shown in Fig. 10. If the decay is linear on a semi-log plot, it has an exponential dependence whose e-folding length is of interest. Thus, based on the particular experimental conditions, four straight lines are drawn on the figure whose slopes correspond to e-folding lengths of  $\lambda_\infty$ ,  $\lambda_{bf}^{(1)}$ ,  $2 \lambda_{bf}$ , and  $\lambda_{fb}$  (taken roughly as  $S_\infty \lambda_{bf}$  - see, e.g., Ref. 16).

- (1) The quantity  $\lambda_{bf}$  is the mean-free-path of a molecule leaving the body in question and colliding with a free-stream molecule. It is defined as :

(see next page)

It is noted that the experimental curves for the wedges with the two smallest values of  $\tau_{L.E.}$  are quite straight, are parallel to one another, and have e-folding lengths of  $\approx 2\lambda_{bf}$ . For the cases involving the larger values of  $\tau_{L.E.}$ , some curvature is evidenced, although restricting one's attention to the region very close to the leading edge, an e-folding length of  $\approx 2\lambda_{bf}$  might still be conjectured. At any rate,  $\lambda_{\infty}$  (which in the general case is not a simple multiple of  $\lambda_{bf}$ ) seems not to be the appropriate scaling length, based on these results and others in which  $\lambda_{bf}/\lambda_{\infty}$  varied from 1.3 to 1.8. In addition, obvious theoretical considerations result in the rejection of  $\lambda_{\infty}$  as an appropriate scaling length for this type of problem and in fact reinforce our feeling that  $\lambda_{bf}$  is a more reasonable choice. We will use  $\lambda_{bf}$  as a normalizing factor in much of what follows and will comment further on its utility later on.

Lines of constant density for wedges with different total angles and leading edge thicknesses (normalized by  $\lambda_{bf}$ ) are shown in Fig. 11 which presents selected examples from a large quantity of data. The contours are determined by appropriate cross-plotting from data used to construct figures similar to Figs. 8 and 9. The influence of  $\tau_{L.E.}$  and  $\omega$  on the disturbance field is clearly seen and follows the expected trends. It would be preferable to draw each contour line with a finite width to illustrate the uncertainty in these results. The positions corresponding to  $\Delta\rho/\rho$  of 2%, 5%, and 10% on the axis for the case

$$\lambda_{bf} = \frac{|\vec{c}_b|}{\sigma(|\vec{v}_{rel}|)n_{\infty}|\vec{v}_{rel}|}$$

where  $\sigma(|\vec{v}_{rel}|)$  is evaluated using the intermolecular potential, derived from viscosity data, given in Ref. 25 at a temperature appropriate to the relative velocity of the colliding species. Its evaluation depends on the angle between colliding species. Under the conditions encountered in these experiments, the value of  $\lambda_{bf}$  for a head-on collision differs by only  $\sim 20\%$  from the value for a right-angle collision and thus an average of the two is employed herein unless otherwise explicitly stated. It should be noted that  $\lambda_{bf}/\lambda_{\infty}$  varied from 1.3 to 1.8 in these experiments.

where the geometric variables are extrapolated to zero ( $\tau_{L.E.} \rightarrow 0$ ;  $\omega \rightarrow 0$ ) are shown in the lower-left square. This point will be discussed later.

In Fig. 12, the variation of  $\Delta\rho/\rho$  with the parameter  $\lambda_{bf}/\tau_{L.E.}$  is presented for two different spatial locations upstream of the leading edge and for three different wedge angles as well as for a flat plate with bevel angle of  $6^\circ$ . Distances are normalized by  $\lambda_{bf}$ . It should be stressed that the values for the abscissa were arrived at by choosing different values of both  $\lambda_{bf}$  (i.e., the results of tests with different  $p_0$ 's) and  $\tau_{L.E.}$  (i.e., the results of tests with different "discs" having the same value of  $\omega$  but various values of  $\tau_{L.E.}$ ). This fact accounts for the greater degree of scatter than is observed on a density map around a single wedge at one specific set of flow conditions. Nevertheless, the trends are clear: a decrease in  $\tau_{L.E.}$  results in a decrease of  $\Delta\rho/\rho$ ; likewise, an increase in  $\omega$  results in an increase of  $\Delta\rho/\rho$ . Note the important influence of  $\tau_{L.E.}$  on  $\Delta\rho/\rho$  even when  $\tau_{L.E.} \ll \lambda_{bf}$ .

Similar plots have been made at nearly a dozen normalized distances upstream of the leading edge. A selected set of such plots is shown in Fig. 13. Again, the striking feature of these plots is the marked influence of the leading edge bluntness on the density disturbance in regions many mean-free-paths upstream from the leading edge. Looking, for instance, at a point ( $x/\lambda_{bf} = 1$ ,  $y/\lambda_{bf} = 2$ ) for  $\omega = 10^\circ$ , it may be concluded that if  $\Delta\rho/\rho$  is to be within  $\sim 20\%$  of its limiting value for  $\tau_{L.E.} \rightarrow 0$ , the ratio  $\lambda_{bf}/\tau_{L.E.}$  must clearly be larger than 50. This implies that the distance from the leading edge at which finite bluntness is no longer important must be much greater than  $100 \tau_{L.E.}$ . In general it may be concluded that  $\lambda_{bf}/\tau_{L.E.}$  must be at least greater than 50 in these experiments if the effect of  $\tau_{L.E.}$  on  $\Delta\rho/\rho$  is to be small.

This conclusion appears to support the conjecture by some researchers (e.g., Ref. 7) that the condition for "sharpness" is much more stringent than simply  $\tau_{L.E.} \ll \lambda_\infty$ . Rather, when one considers the relative role played by the blunt

leading edge and the upper (and lower) surfaces of a plane plate, taking into account angular effects, the condition  $\tau_{L.E.} \ll \lambda_{bf}/S_{\infty}$  seems theoretically more valid. As our results suggest that  $\lambda_{bf}/\tau_{L.E.}$  must be clearly greater than 50 (perhaps as large as 100) before the influence of  $\tau$  on  $\Delta\rho/\rho$  upstream is negligible for the case of  $S_{\infty} \approx 7$ ; i.e.,  $(\tau_{L.E.} S_{\infty}/\lambda_{bf})_{exp} \ll \mathcal{O}(0.1)$ ; they lend support to this more stringent criterion.

Some caution must be observed in assessing these results, however. The smallest values of  $\lambda_{bf}$  are of the same order as the diameter of the electron beam; thus data points in regions of large gradients must be considered as representing some kind of overall average value for the quantity  $\Delta\rho/\rho$ . In addition, the models with the minimum leading edge thickness ( $\sim 0.05$  mm) may have been characterized by a variation in leading edge thickness of as much as  $\pm 0.01$  mm. The data points corresponding to these values of  $\tau_{L.E.}$  thus are representative of some kind of average value for  $\tau_{L.E.}$  where the stress is on the word average. In our opinion, neither of these factors could be responsible for a qualitative change in the results. However, a precise quantitative interpretation of the data is probably not justified, particularly when  $\Delta\rho/\rho \leq 2\%$ .

The upstream influence of an infinitely-thin flat plate can be determined in principle by extrapolating the results of the wedge data to the limits of  $\omega \rightarrow 0$  and  $\tau_{L.E.} \rightarrow 0$ . Since only three wedge angles ( $6^\circ$ ,  $10^\circ$ , and  $20^\circ$ ) were examined in this study, and since a variation in  $\Delta\rho/\rho$  with  $\tau_{L.E.}$  at a given station is still observed for  $\lambda_{bf}/\tau_{L.E.} \geq 50$ , the conclusions of such an extrapolation must be viewed with caution. However, they do represent the first experimental results which can be compared unambiguously with existing theoretical treatments (e.g., Refs. 7 and 9), all of which are valid only for the infinitely-thin flat plate. The extrapolated values for  $\Delta\rho/\rho$  at three different upstream locations are shown in the lower left graph on Fig. 11 and are cited on the next page :

$\Delta\rho/\rho$	$x/\lambda_{bf}$
$\sim 2\%$	2.1-2.3
$\sim 5\%$	1.0-1.2
$\sim 10\%$	0.1-0.3

The results apply only to the particular experimental conditions in question (unless of course  $\lambda_{bf}$  is an all-inclusive correlation parameter, a point which has certainly not yet been proved); i.e.  $6 < M_\infty < 11$  (primarily at  $M_\infty = 9$ ) and  $T_b = T_0$ .

To put the results of the upstream influence measurements into a form useful to other experimenters, Fig. 14 has been prepared which shows the normalized spatial location of the "5%" disturbance point (i.e.,  $\Delta\rho/\rho = 5\%$ ) upstream of a wedge as a function of leading edge thickness and wedge total angle. For given wedge geometry (specified by  $\omega$  and  $\tau_{L.E.}$ ), the graph shows the axial distance at which a measurable (i.e.,  $\sim 5\%$ ) disturbance is found. More importantly, the graph indicates the strong coupling that exists between  $\tau_{L.E.}$  and  $\omega$ . Certain generalizations can be made for limiting cases. If  $\lambda_{bf}/\tau_{L.E.} > 10$ , then a variation in  $\lambda_{bf}/\tau_{L.E.}$  produces a relatively minor effect on the upstream disturbance for values of  $\omega > 15^\circ$  or  $20^\circ$ ; i.e., the wedge angle dominates. For  $\omega$  to have a small effect on  $\Delta\rho/\rho$ , it is clearly seen that it must be much less than  $5^\circ$ , but the value of  $\lambda_{bf}/\tau_{L.E.}$  must be specified within a certain range before a more precise statement can be made.

An extrapolation of the experimental results to  $\omega \rightarrow 0$  and  $\tau_{L.E.} \rightarrow 0$  indicates as seen in Fig. 11 that the "5%" disturbance point will be found at  $x/\lambda_{bf} = 1$ . Thus, a geometry as extreme (from the machining point-of-view) as  $\lambda_{bf}/\tau_{L.E.} = 50$  and  $\omega = 10^\circ$  (see Fig. 14) will produce a "5%" disturbance at an upstream distance twice that of the  $\omega = 0$ ,  $\tau_{L.E.} = 0$  (infinitely-thin flat plate) case.

Figure 14 may also be used in another fashion. Since each of the two curves represents the spatial location



for a "5%" disturbance, a particular experiment, corresponding to given  $\lambda_{bf}$ ,  $\tau_{L.E.}$ , and  $\omega$ , will specify a point on the plot which in general will not coincide with one of the two curves. If the point lies to the right and below a curve corresponding to a given value of  $x/\lambda_{bf}$ , it means that the density disturbance at the given value of  $x/\lambda_{bf}$  will be more than 5%. Conversely, if the point lies above and to the left of the curve, the density disturbance will be less than 5% at the given value of  $x/\lambda_{bf}$ . Thus, the figure may serve as an approximate design chart.

### C. Comparisons with other Results

A precise comparison of the results presented in this report with the work of other researchers is difficult because few studies have been made with a wedge and none, to our knowledge, have dealt with the upstream influence of such a shape. That the upstream influence of a wedge of total angle  $\omega$  is different from that of a flat plate of bevel angle  $\omega$  is clear on physical grounds (the latter is characterized by an asymmetric transverse density profile with a maximum value lying below the plane of the plate) and is demonstrated experimentally on Figs. 12 and 13 for the case of  $\omega = 6^\circ$ . Nevertheless, a few general comparisons can be drawn.

Joss and Bogdonoff (Ref. 4) find, for the case  $\omega = 20^\circ$  and  $\lambda_{bf}/\tau_{L.E.} = 30$  (where we have computed on the basis of their flow conditions that  $\lambda_{bf}/\lambda_\infty = 1.6$ ), that  $\Delta\rho/\rho = 12\%$  at  $x/\lambda_{bf} = 3$ . For a wedge having the same geometric parameters, we find  $\Delta\rho/\rho = 6\%$  at  $x/\lambda_{bf} = 3$ . Since we have shown that  $\Delta\rho/\rho$  will increase significantly if a wedge of total angle  $\omega$  is transformed to a flat plate of bevel angle  $\omega$ , their results are not inconsistent with ours. (A similar halving of  $\Delta\rho/\rho$  is found at  $x/\lambda_{bf} = 1$  as well : from  $\sim 50\%$  to  $\sim 25\%$ ).

Lillicrap and Berry (Ref. 12) studied the flow field around a  $15^\circ$  bevel-angle flat plate with  $\lambda_{bf}/\tau_{L.E.} = 35$  (for their case, we compute  $\lambda_{bf}/\lambda_\infty = 0.8$ ). They find  $\Delta\rho/\rho = 5\%$  at a value of  $x/\lambda_{bf} = 2.5$  and a  $\Delta\rho/\rho = 20\%-30\%$  at  $x/\lambda_{bf} = 1$ .

An examination of Figs. 13 and 14 (recalling again that these graphs apply only to a wedge) also shows their results to be consistent with our findings.

In Hickman's experiments (Ref. 2), the upstream field of his  $10^\circ$  bevel-angle flat plate is unchanged when he replaces his model with a thin sheet ( $\tau_{L.E.} = 0.05$  mm) under tension. As he does not quote the thickness of his flat plate it cannot be determined whether both models might have produced nearly the same disturbance simply because they were characterized by similar values of  $\tau_{L.E.}$ . Nevertheless, the scatter in his results in the vicinity of the leading edge where  $\Delta\rho/\rho$  is of order 10% eliminates any possibility of conclusively settling this point. (An absolute accuracy of  $\pm 5\%$  for  $\rho$  is quoted; thus the value of  $(\Delta\rho/\rho)_{\text{leading edge}}$  could range from 5% to 15%.)

In the previous section, extrapolated results for the case  $\omega \rightarrow 0$ ,  $\tau_{L.E.} \rightarrow 0$  (the infinitely-thin flat plate) were presented. It is of interest to compare these results with those obtained by other experimenters at  $x/\lambda_{bf} = 1$ . Fortunately,  $\lambda_{bf}/\tau_{L.E.} \approx 30-35$  for each of the following cases :

	$\omega$	$\tau_{L.E.}$	$\Delta\rho/\rho$ at $x/\lambda_{bf} = 1$
J+B (Ref. 4)	$20^\circ$	0.025 mm	$\sim 50\%$
L+B (Ref. 12)	$15^\circ$	$\sim 0.01$ mm	20-30%
H* (Ref. 2)	$10^\circ$ and $0^\circ$	0.05 mm (for $0^\circ$ case)	5-10%
Present (extra- polated)	$0^\circ$	0	$\sim 5\%$

\* Hickman does not specify  $\tau_{L.E.}$  for his  $10^\circ$  wedge. He concludes, as discussed earlier, that the upstream disturbance for the two cases reported was the same.

The results follow a logical trend and illustrate the difficulty in producing an experimental situation which approximates the theoretical case of an infinitely-thin flat plate.

It was mentioned earlier that one set of density profiles was recorded for the case of a flat plate with a  $6^\circ$  bevel angle and a  $\lambda_{bf}/\tau_{L.E.} = 15$ . This test was carried out so that a direct comparison of our results could be made with those obtained by other investigators who have concentrated on the flat plate problem. The region examined was from 3 to 4  $\lambda_{bf}$ 's upstream to 12  $\lambda_{bf}$ 's downstream of the leading edge. (Some data were recorded for values of  $\lambda_{bf}/\tau_{L.E.}$  as large as 75, but only extend to 2-3  $\lambda_{bf}$ 's downstream of the leading edge). A "5%" disturbance line (which might be called the boundary of the disturbance region) was then constructed.

Vogenitz, et. al. (Ref. 7) have compared their Monte Carlo (M.C.) results (see their Fig. 6) in the format of a 5% density disturbance line on a  $(x/\lambda_\infty, y/\lambda_\infty)$  diagram with the results obtained by Joss, Vas and Bogdonoff (Ref. 26) and Becker (Ref. 13). The former data show poor agreement with the M.C. results, but this may have been due to an unfortunate choice of data because a later paper by Joss and Bogdonoff (Ref. 4) presents results which show reasonably good agreement ( $\pm 10\%$ ) with the M.C. results, except near the leading edge where the experimental results show a thicker disturbance region. Our data and that of Lillcrap and Berry (Ref. 12) show a "5%" disturbance extending much farther away from the plate than predicted by the M.C. theory (roughly 75-100% in the former case and 25-35% in the latter case). Note that our data represent a "hot-wall" case ( $T_b = T_0$ ), Lillcrap and Berry's a "cool-wall" case ( $T_b = 0.5 T_0$ ), and Joss and Bogdonoff's a "cold-wall" case ( $T_w = 0.25 T_0$ ). The M.C. results were computed for the case  $T_b = 0.08 T_0$ ; i.e., a cold wall case.

If all the data are presented in terms of distances normalized by  $\lambda_{bf}$  instead of  $\lambda_\infty$ , the agreement becomes significantly better, as shown in Fig. 15. Our data are presented in a band to illustrate the degree of uncertainty we feel should be applied to the results. Except for the data of Jos and Bogdonoff

(Ref. 4), which now define a thinner disturbance region, the remaining data show remarkably good agreement considering the wide variation in flow conditions. From these results we conclude that  $\lambda_{bf}$  is a more appropriate variable than  $\lambda_{\infty}$  to characterize the extent of the disturbance region in the vicinity of the leading edge.

The quantity  $\lambda_{fb}$ , which is roughly equal to  $S_{\infty}\lambda_{bf}$  for the flat plate geometry, has also been discussed as a useful correlation parameter when examining the relaxation of the free stream molecules as they pass through a cloud of body molecules (Ref. 16). This picture suggests that distance normal to the flat plate should continue to be normalized by  $\lambda_{bf}$ , but that distances parallel to the plate might be normalized by  $\lambda_{fb}$ . The results are shown in Fig. 16. A major improvement in correlation over roughly one  $\lambda_{fb}$  is seen to occur, particularly with respect to the Jos and Bogdonoff (Ref. 4) results. The upstream region is less well correlated, but perhaps it should be considered as part of the disturbance field and therefore perhaps the upstream distances should be normalized by  $\lambda_{bf}$  as before.

The agreement between the experimental results (all for a diatomic gas -  $N_2$ ) and the M.C. results (monatomic - hard sphere) are probably to some extent fortuitous, although one might be tempted to argue that a quantity such as density - particularly when one is looking for the spatial location of a weak disturbance boundary - should not be strongly influenced by molecular structure.

Some caution must be shown in evaluating the results shown in Figs. 15 and 16 because of the necessity to convert the conditions employed by other researchers into the parameter  $\lambda_{bf}$ . It is believed that the conversion factors are at best only approximately correct, but they are at least self-consistent.

## CONCLUSIONS

An experimental study was performed to determine the nature of the disturbance to the free stream density in the vicinity of the leading edge of a wedge. A number of wedge angles and leading edge thicknesses were chosen so as to examine the effect of geometry. The development of a modulation technique, wherein a two-dimensional wedge was transformed into a spinning four-sector disc, allowed the quantity  $\Delta\rho = \rho(x,y) - \rho_\infty$  to be measured directly with an accuracy comparable to that normally attained in a measurement of  $\rho$ . The experiments were performed in a free jet flow field.

The principal conclusions drawn from the results of this study are :

1. The mean-free-path of a molecule leaving the body and colliding with a free-stream molecule,  $\lambda_{bf}$ , appears to be the most satisfactory scaling length in the upstream region.
2. The criterion for a negligible influence of leading edge thickness on the upstream density is more severe than earlier realized. A ratio of  $\lambda_{bf}/\tau_{L.E.} > 50$  (even for wedge angles of only  $6^\circ$ ) is required to bring  $\Delta\rho/\rho$  to within  $\sim 20\%$  of the limiting value found when  $\tau_{L.E.} \rightarrow 0$ . The criterion,

$$\tau_{L.E.} \ll \lambda_{bf}/S_\infty,$$

valid on physical grounds for a flat plate appears to be confirmed, but further experiments at much larger Mach numbers are still necessary to furnish final proof.

3. A strong coupling exists between wedge angle and leading edge thickness. Unless  $\alpha$  is less than  $5^\circ$ , it appears nearly impossible to reduce the upstream influence to the values representative of a truly infinitely-thin flat plate

simply by adjusting the leading edge thickness. Although such a finding, in conjunction with the conclusion above, casts doubt on the applicability of virtually all measurements previously made within a few mean-free-paths downstream of the leading edge of a flat plate; it should be stressed that the effect of an upstream disturbance, which differs from that due to an infinitely-thin flat plate, on the downstream properties of interest is not known at present.

4. A qualitative chart predicting the extent of upstream disturbance as a function of  $\lambda_{bf}/\tau_{L.E.}$  and  $\omega$  is now available for use by other researchers. It holds for the case of a wedge; however, it sets a lower limit for the flat-plate case as well because the on-axis disturbance from a flat plate is always larger than for a wedge with the same values of  $\omega$  and  $\tau_{L.E.}$ .

5. Limiting on-axis values for  $\Delta\rho/\rho$  corresponding to  $\omega \rightarrow 0$   $\tau_{L.E.} \rightarrow 0$  (the infinitely-thin flat plate case) as a function of position have been determined :

$\Delta\rho/\rho, \%$	$x/\lambda_{bf}$
$\sim 2$	2.1 - 2.3
$\sim 5$	1.0 - 1.2
$\sim 10$	0.1 - 0.3

6. It is tentatively concluded that  $\lambda_{bf}$  is the correct scaling length for the disturbance region upstream and above a flat plate in a region which extends  $\sim 1 \lambda_{fb}$  downstream from the leading edge. This conclusion appears valid for cold-wall and hot-wall hypersonic flows.

7. The Monte Carlo treatment for the case of an infinitely-thin flat plate predicts limits for the density disturbance region which agree with measurements when  $\lambda_{bf}$  and  $\lambda_{fb}$  are used to normalize, respectively, the coordinates perpendicular and

parallel to the plate surface.

The following limitations to this study should be kept in mind :

1. The model was a disc and thus only approximated a 2-D wedge. However, the measurement zone was small compared to the disc radius.
2. The flow field was a source flow, not a parallel flow. Although all  $\Delta p$ 's were normalized by the local value of  $\rho_\infty$ , molecules reflected upstream were moving into a region of increasing  $\rho_\infty$ .
3. The transformation of data expressed in terms of  $\lambda_\infty$  to data expressed in terms of  $\lambda_{bf}$  may be dangerous when all flow conditions are not precisely known. The results presented by some researchers may have been inadvertently misrepresented herein for this reason.

## REFERENCES

1. Becker, M. and Boylan, D.E. : "Experimental Flow Field Investigations near the Sharp Leading Edge of a Cooled Flat Plate in a Hypervelocity, Low-Density Flow", Rarefied Gas Dynamics, Suppl. 4, edited by C.L. Brundin, Academic Press, New York, 1967, pp. 993-1014 (also see AFDC-TR-66-111).
2. Hickman, R.S. : "Hypersonic Transitional Flow at the Leading Edge of a Sharp Flat Plate", Rarefied Gas Dynamics, Suppl. 5, edited by L. Trilling and H.Y. Wachman, Academic Press, New York, 1969, pp. 583-592.
3. Hickman, R.S. : "Density Flow near a Wedge in Rarefied Flow", Phys. Fluids, 13, December 1970, pp. 3051-2 (RN)
4. Joss, W.W. and Bogdonoff, S.M. : "A Detailed Study of the Flow around the Leading Edge of a Flat Plate in Hypersonic Low Density Flow", Rarefied Gas Dynamics, Suppl. 5, edited by L. Trilling and H.Y. Wachman, Academic Press, New York, 1969, pp. 483-492.
5. Joss, W.W. and Bogdonoff, S.M. : "An Experimental Study of the Effects of Small Leading Edge Thickness on the Development of the Hypersonic Rarefied Flow over a Flat Plate", Presented at 7th Int'l Symposium on Rarefied Gas Dynamics, Pisa, 1970.
6. Vidal, R.J., Merritt, G.E. and Bartz, J.A. : "Flowfield Surveys in the Leading Edge Region of a Sharp Flat Plate", Presented at 7th Int'l Symposium on Rarefied Gas Dynamics, Pisa, 1970 (also AFOSR-TR-71-0828).
7. Vogenitz, F.W., Broadwell, J.E. and Bird, G.A. : "Leading Edge Flow by the Monte Carlo Direct Simulation Technique", AIAA Jour., Vol. 8, No. 3, March 1970, pp. 504-510.
8. Charvat, A.F. : "Molecular Flow Study of the Hypersonic Sharp Leading Edge Interaction", Rarefied Gas Dynamics, Suppl. 1, edited by L. Talbot, Academic Press, New York, 1961, pp. 553-540.
9. Huang, A.B. and Hwang, P.F. : "Kinetic Theory of the Sharp Leading Edge Problem. II. Hypersonic Flow", Presented at the 19th Congress of the Int. Astron. Fed., New York, October 1968.
10. Vidal, R.J. and Bartz, J.A. : "Surface Measurements on Sharp Flat Plates and Wedges in Low-Density Hypersonic Flow", AIAA Jour., Vol. 7, No. 6, June 1969.



11. Metcalf, S.C., Lillicrap, D.C. and Berry, C.J. : "A Study of the Effect of Surface Temperature on the Shock-Layer Development over Sharp-Edged Shapes in Low-Reynolds-Number High Speed Flow", Rarefied Gas Dynamics, Suppl. 5, Vol. 1, edited by L. Trilling and H.Y. Wachman, Academic Press, New York, 1969, pp. 619-634.
12. Lillicrap, D.C. and Berry, C.J. : "Experimental Model for High-Speed Rarefied Flow over a Sharp Flat Plate", Phys. Fluids 13, pp. 1146-1152, May 1970.
13. Becker, M. : "Flat Plate Flow Field and Surface Measurements from Merged Layer into Transition Regime", Rarefied Gas Dynamics, Suppl. 5, edited by L. Trilling and H.V. Wachman, Academic Press, New York, 1969, pp. 515-528.
14. Horstman, H.H. : "Number Flux Measurements on Sharp Flat Plates and Wedges in the Kinetic Flow Regime", Presented at 7th Int'l Symp. on Rarefied Gas Dynamics, Pisa, 1970.
15. Lewis, J.H. and Smith, J.A. : "Surface Molecular Flux, Density, and Pressure on a Sharp Flat Plate in Rarefied Hypersonic Flow", Presented at 7th Int'l Symp. on Rarefied Gas Dynamics, Pisa, 1970.
16. Hamel, B.B., and Cooper, A.L., "A First Collision Theory of the Hyperthermal Leading Edge Problem" Rarefied Gas Dynamics, Suppl. 5, edited by L. Trilling and H.V. Wachman, Academic Press, New York, pp. 433-440.
17. Yoshizawa, Y. : "The Sharp Leading Edge Problem by a Monte Carlo Technique", Presented at the 7th Int'l Symp. on Rarefied Gas Dynamics, Pisa, 1970.
18. Muntz, E.P. : "The Electron Beam Fluorescence Technique", AGARDograph 132, December 1968.
19. Smolderen, J.J. and Wendt, J.F. : "The Low Density Wind Tunnel and Associated Research Program at the von Karman Institute for Fluid Dynamics" Presented at the Symposium "Surface-Vacuum-Space", Liège, Belgium, April 1971. Published in Vacuum-Technik, No. 8, November 1971.
20. Ashkenas, H. and Sherman, F.S. : "The Structure and Utilization of Supersonic Free Jets in Low Density Wind Tunnels", Rarefied Gas Dynamics, Suppl. 3, edited by J.H. de Leeuw, Academic Press, New York, 1965.

21. Bier, K. and Hagena, O. : "Optimum Conditions for Generating Molecular Beams by Nozzles", Rarefied Gas Dynamics, Suppl.3, edited by J.H. de Leeuw, Academic Press, New York, 1965.
22. Sherman, F.S. : "A Source Flow Model of Viscous Effects in Hypersonic Axi-Symmetric Free Jets", 6th Symposium on Advanced Problems in Fluid Mechanics, Archivum Mechaniki Stosowanej 2, 16, 1964.
23. Knuth, E.L. : "Rotational and Translational Relaxation Effects in Low-Density Hypersonic Free Jets", University of California, UCLA Dept. of Engineering Report No. 64-53, November 1964.
24. Marrone, P.V. : "Temperature and Density Measurements in Free Jets and Shock Waves", Phys. Fluids, 10, March 1967, pp. 521-538 (also see UTIAS Report 113).
25. Hirschfelder, J.O., Curtiss, C.F. and Bird, R.B. : "Molecular Theory of Gases and Liquids", John Wiley and Sons, Inc., New York, 1954.
26. Joss, W.W., Vas, I.E., and Bogdonoff, S.M., "Studies of the Leading Edge Effect on the Rarefied Hypersonic Flow over a Flat Plate" AIAA Paper No. 68-5, presented at Sixth Aerospace Sciences Meeting, New York, January 22-24, 1968.

TABLE 1    EXPERIMENTAL CONDITIONS

A. WEDGE GEOMETRY

Model No.	$\omega$	$\tau_{L.E.}$ (mm)
1	10.35°	0.09
2	10.5°	0.39
3	10.15°	0.046
4	10.3°	0.9
5	19.8°	0.36
6	6.3°	0.085

TABLE 1 EXPERIMENTAL CONDITIONS (Cont'd)

B. TEST CONDITIONS

Test no.	$P_0$ (Torr)	x/D	$M_\infty^*$	$S_b^*$	$\lambda_\infty^*$ (mm)	$\bar{\lambda}_{of}^*$ (mm)	$\delta M/M^*, \%$ /mm	Extent of upstream test region, mm
A	5	5	6.3	1.75	1.0	1.25	1.4	5
B	5	10	8.7	1.81	3.0	5.1	0.7	6
C	10	5	6.3	1.75	0.5	0.625	1.4	5
D	10	10	8.7	1.81	1.5	2.55	0.7	6
E	25	10	8.7	1.81	0.6	1.0	0.7	6
F	25	17	11	1.83	1.4	2.38	0.4	6

\* evaluated at leading edge

TABLE 1 EXPERIMENTAL CONDITIONS (Cont'd)

C. EXPERIMENTAL PROGRAM

	A	B	C	D	E	F
1	X	X	X	X	X	
2	X	X	X	X	X	X
3		X		X	X	
4		X			X	
5		X		X	X	
6		X		X	X	
6(2)		X		X	X	

(2)

Asymmetric wedge; i.e. flat plate with bevel angle of 6°

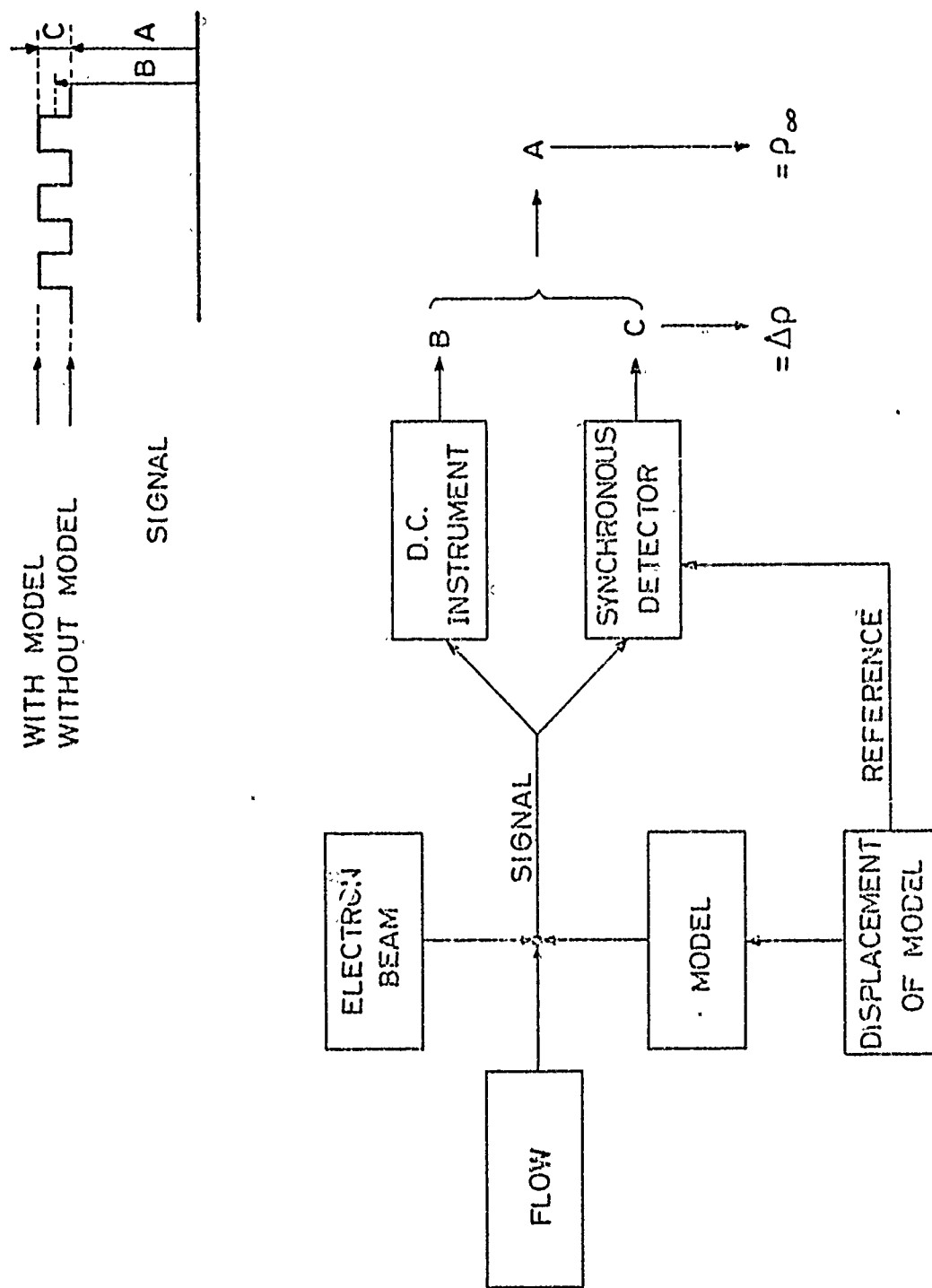
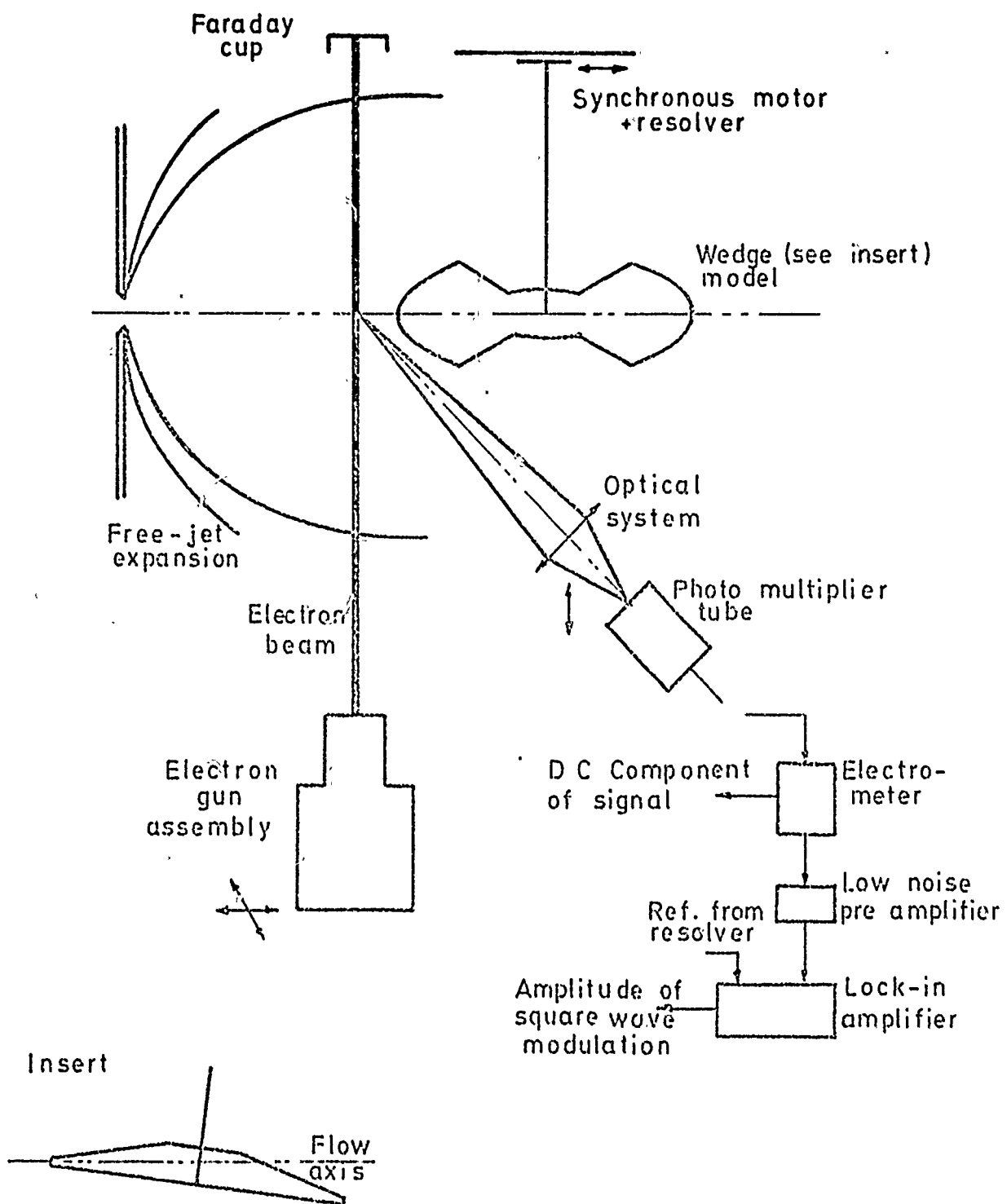


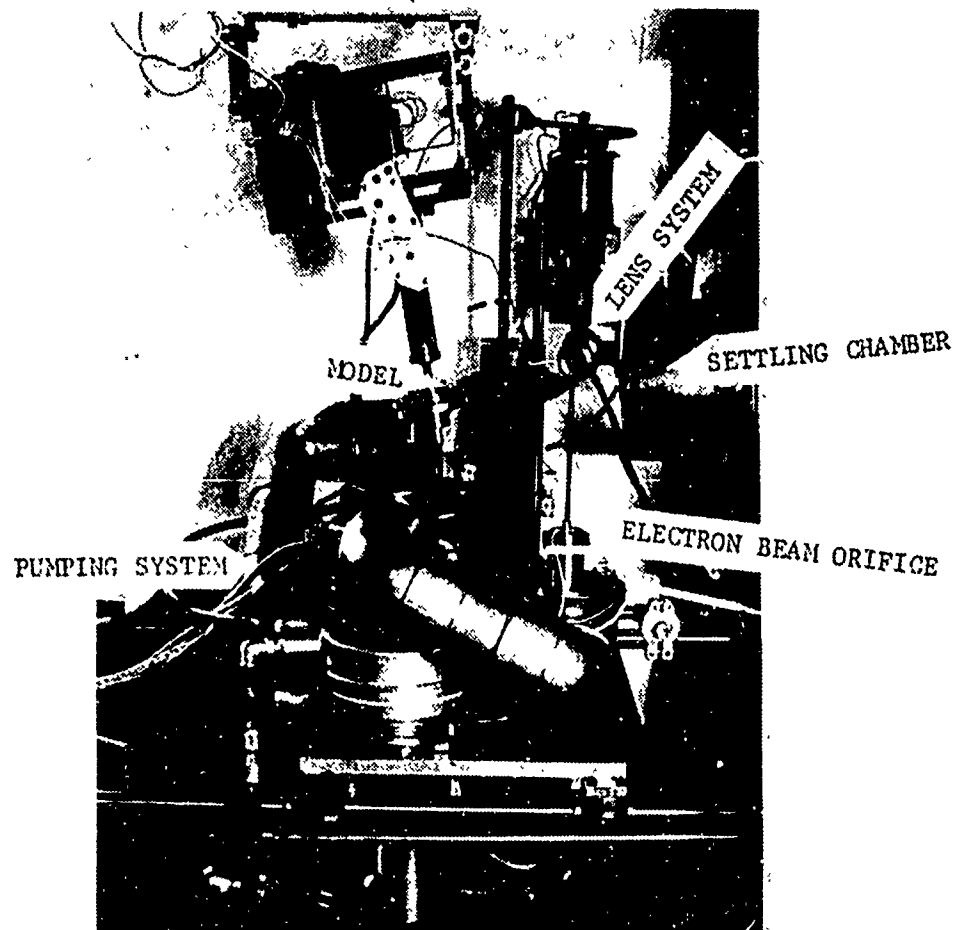
Figure 1

PRINCIPLE OF THE MODULATION TECHNIQUE FOR  
DENSITY DISTURBANCE MEASUREMENTS.



SCHEMATIC FOR DENSITY DISTURBANCE MEASUREMENTS IN LEADING EDGE REGION

Figure 2



EXPERIMENTAL ARRANGEMENT

Figure 3



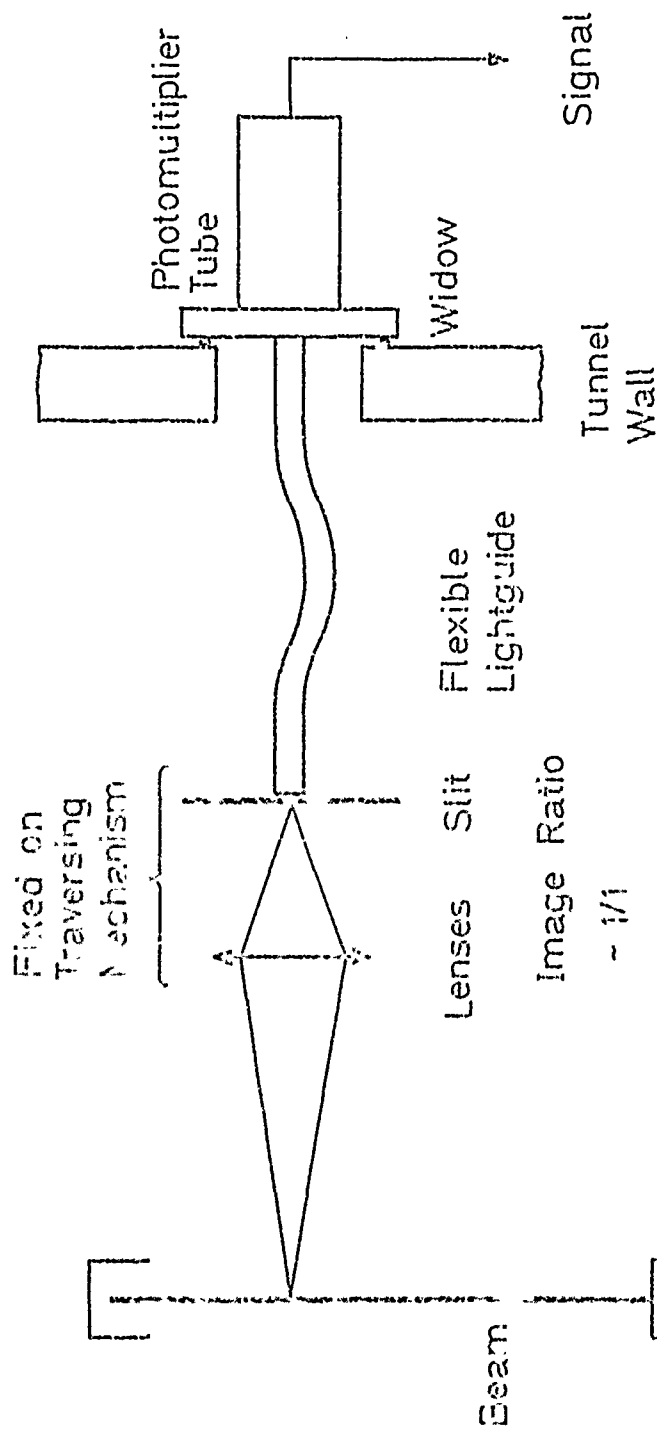
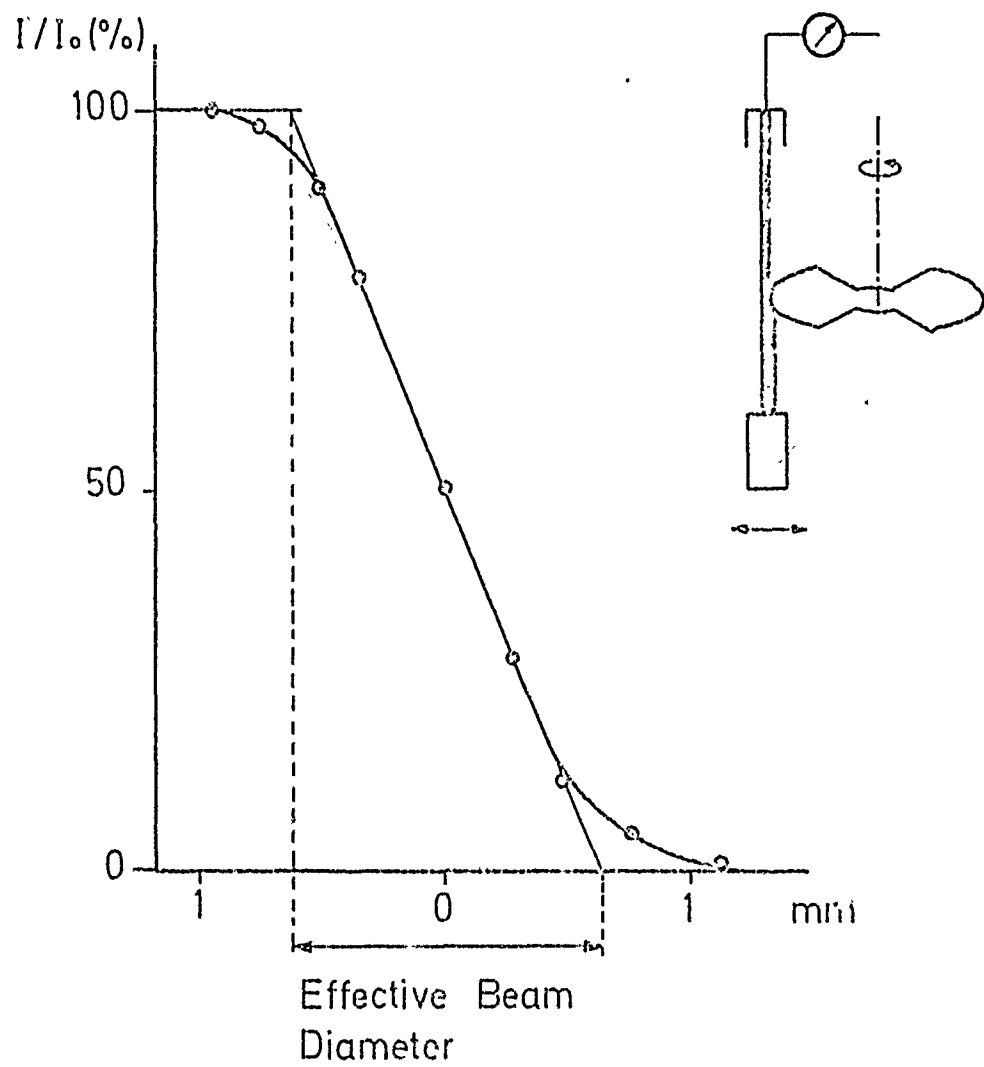


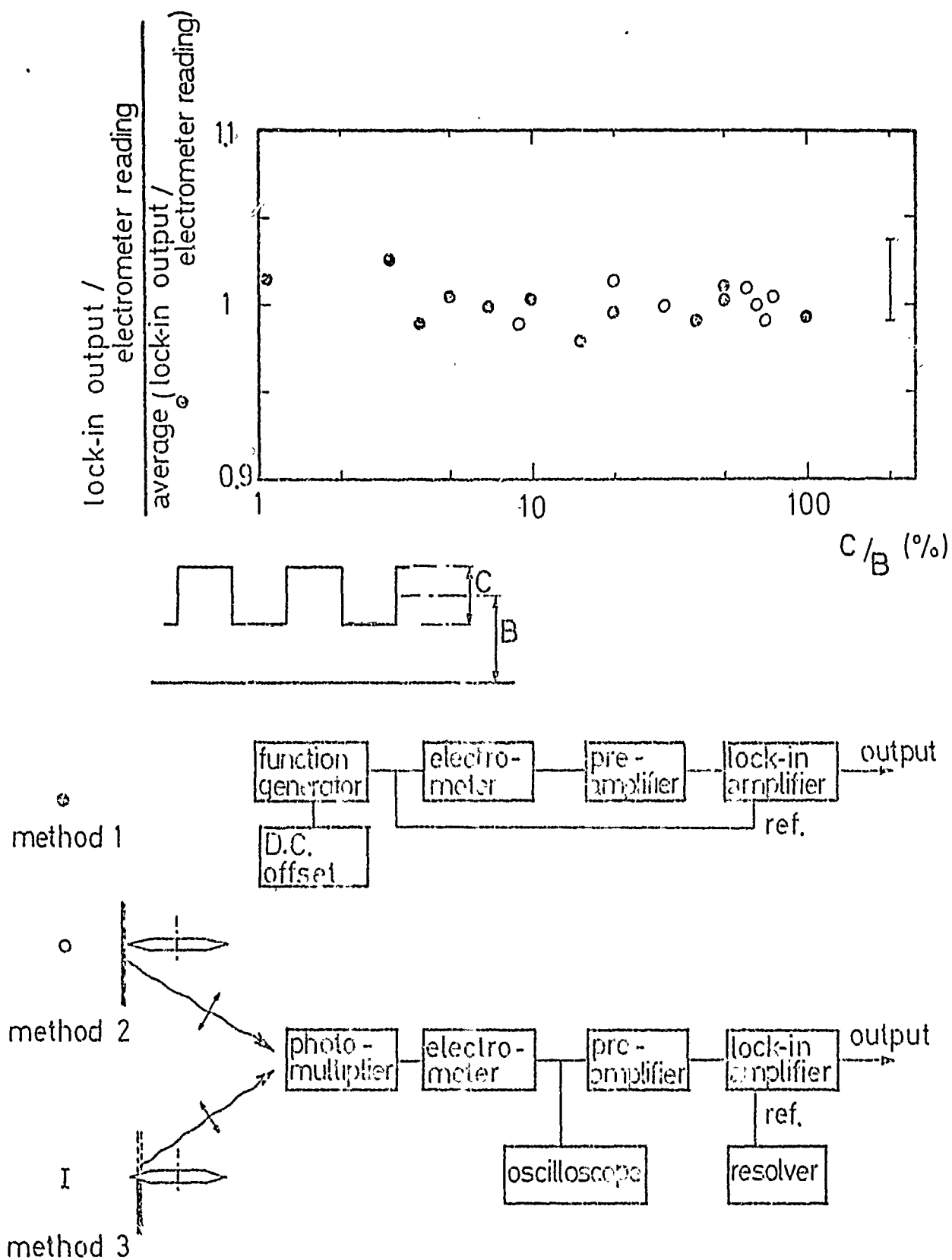
Figure 4

ARRANGEMENT OF THE OPTICAL SYSTEM



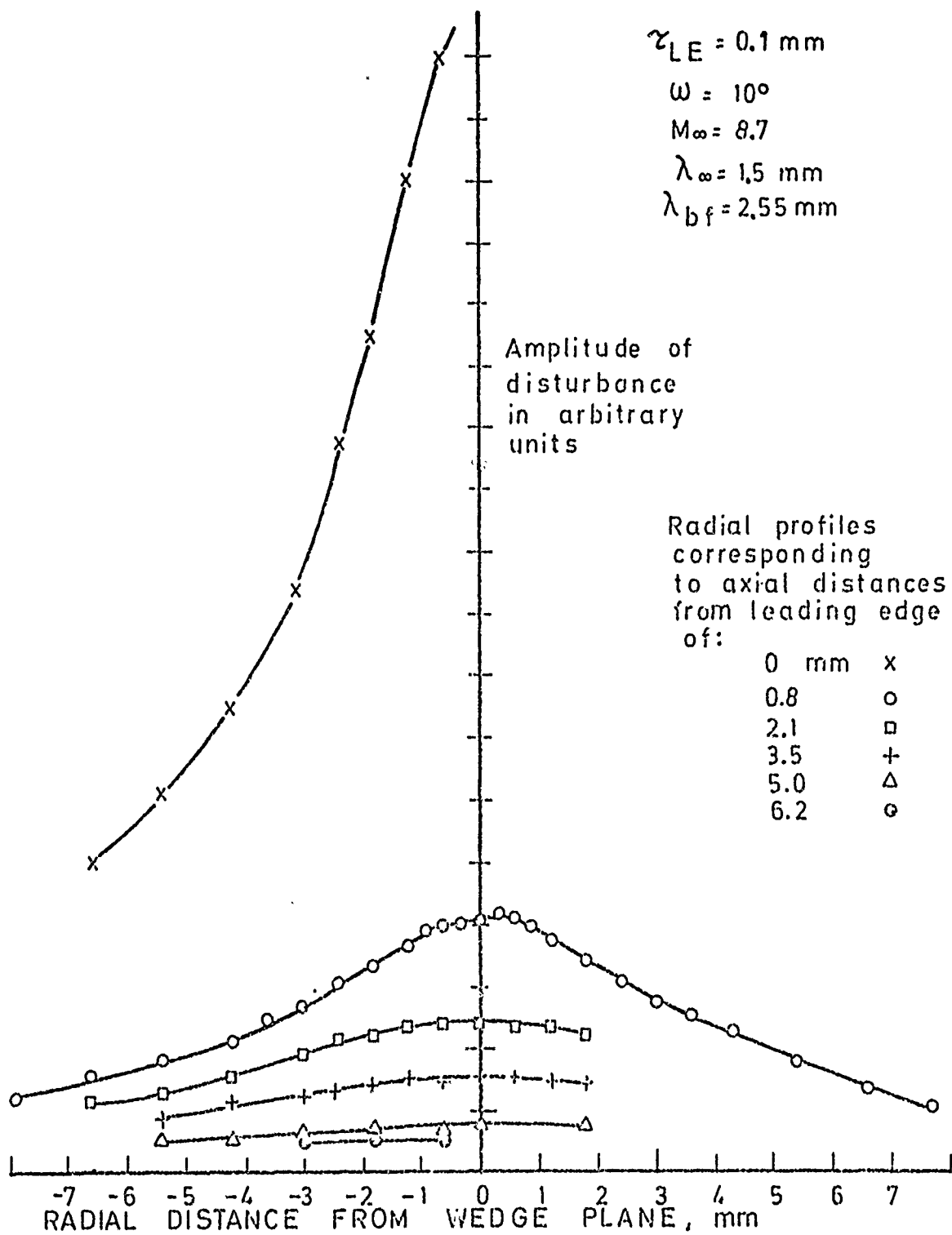
DETERMINATION OF THE EFFECTIVE  
BEAM DIAMETER

Figure 5



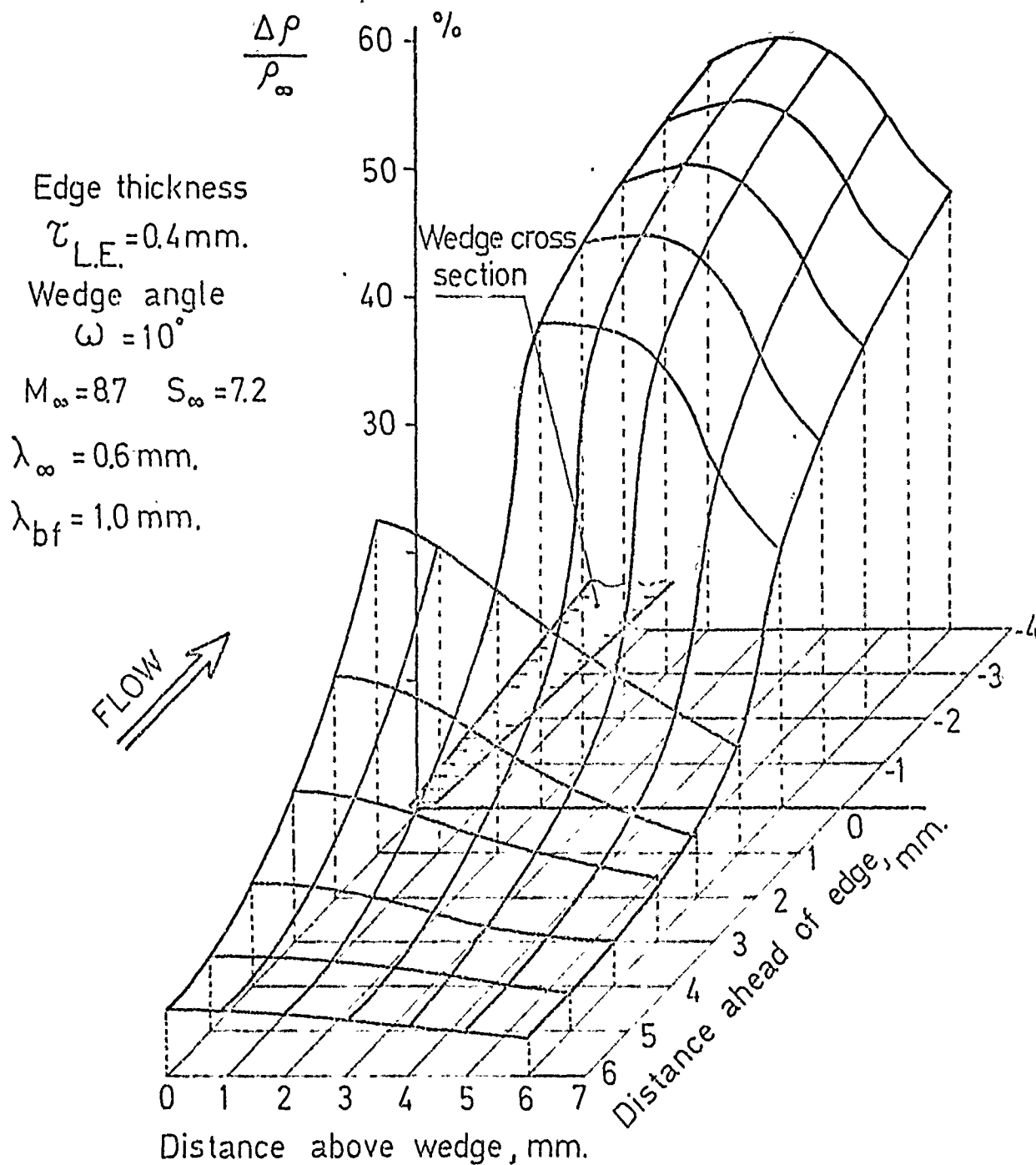
## CALIBRATION METHODS AND RESULTS

Figure 6



RADIAL PROFILES OF EXPERIMENTAL DATA  
 PROPORTIONAL TO DENSITY DISTURBANCE  $\Delta\rho$

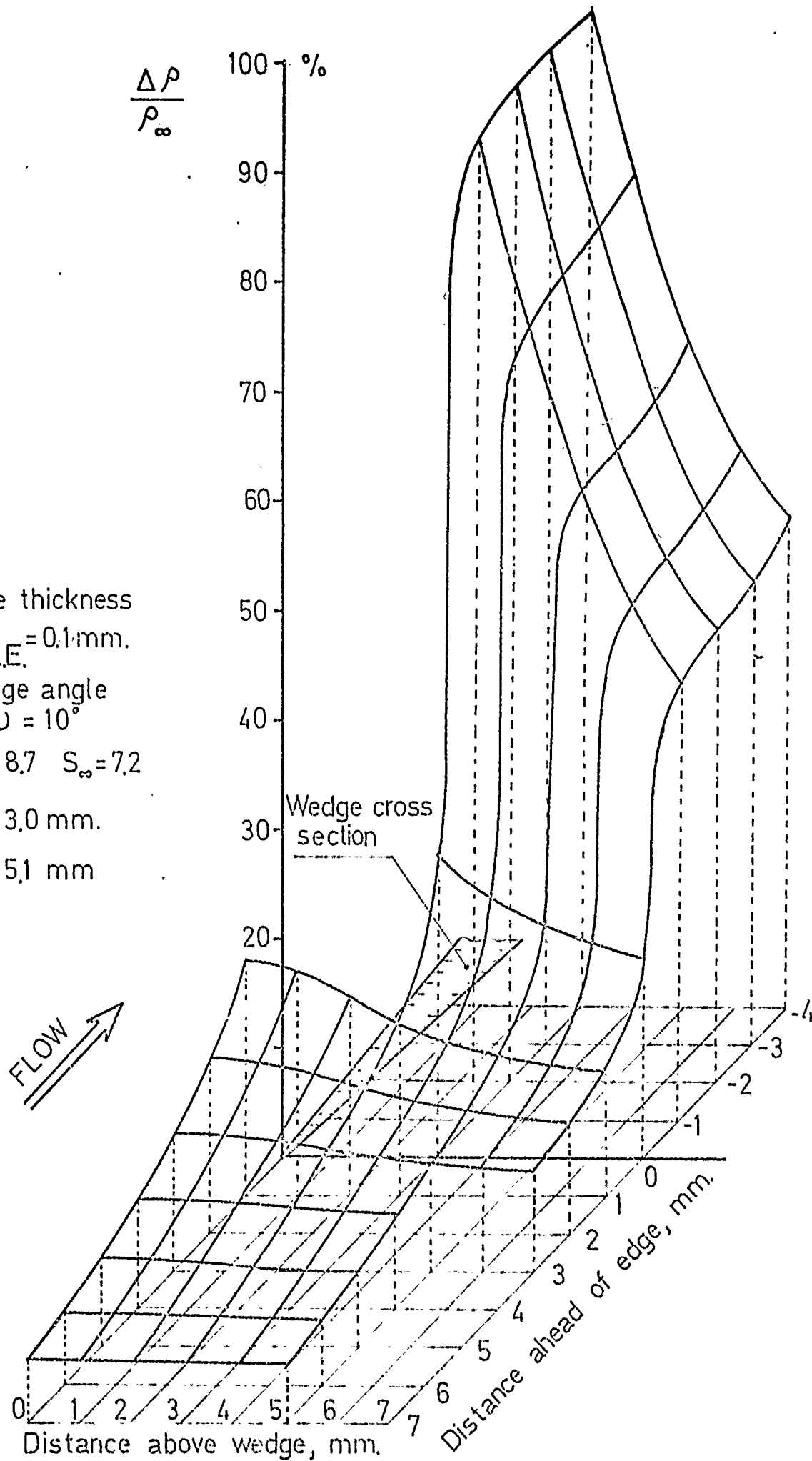
Figure7



DENSITY DISTURBANCE IN LEADING EDGE  
 REGION

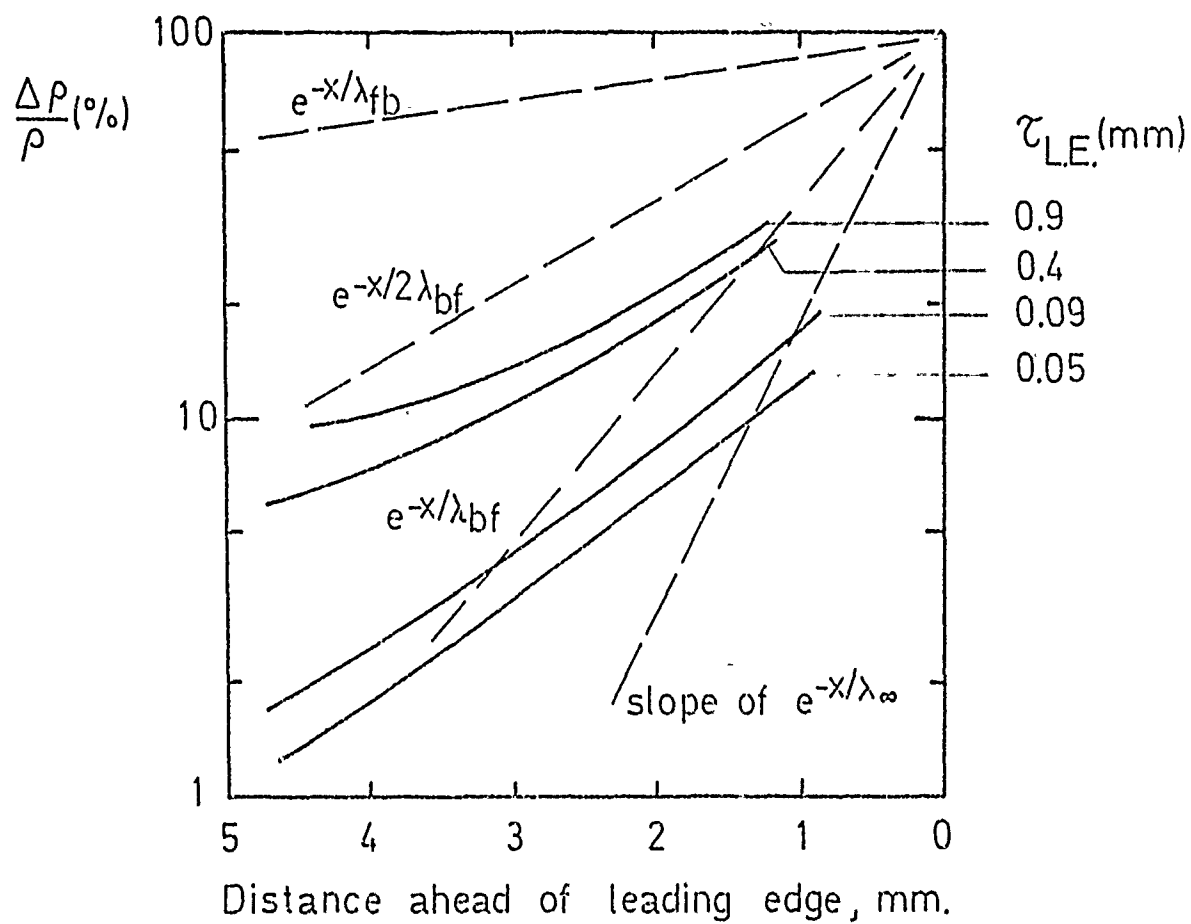
Figure 8

Edge thickness  
 $\tau_{L.E.} = 0.1 \text{ mm.}$   
 Wedge angle  
 $\omega = 10^\circ$   
 $M_\infty = 8.7 \quad S_\infty = 7.2$   
 $\lambda_\infty = 3.0 \text{ mm.}$   
 $\lambda_{bf} = 5.1 \text{ mm}$



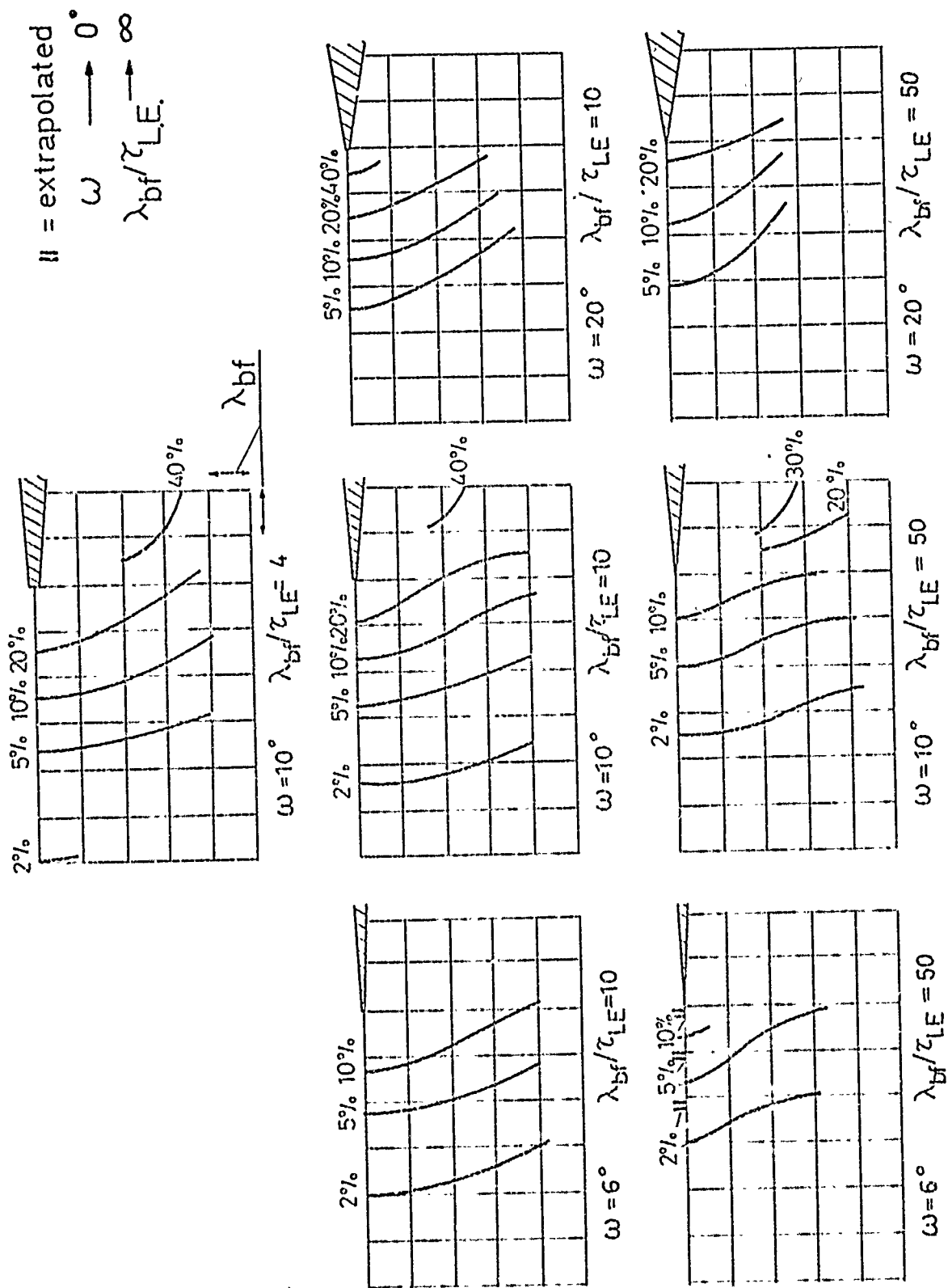
DENSITY DISTURBANCE IN LEADING EDGE REGION

Figure 9



ON-AXIS UPSTREAM DISTURBANCE

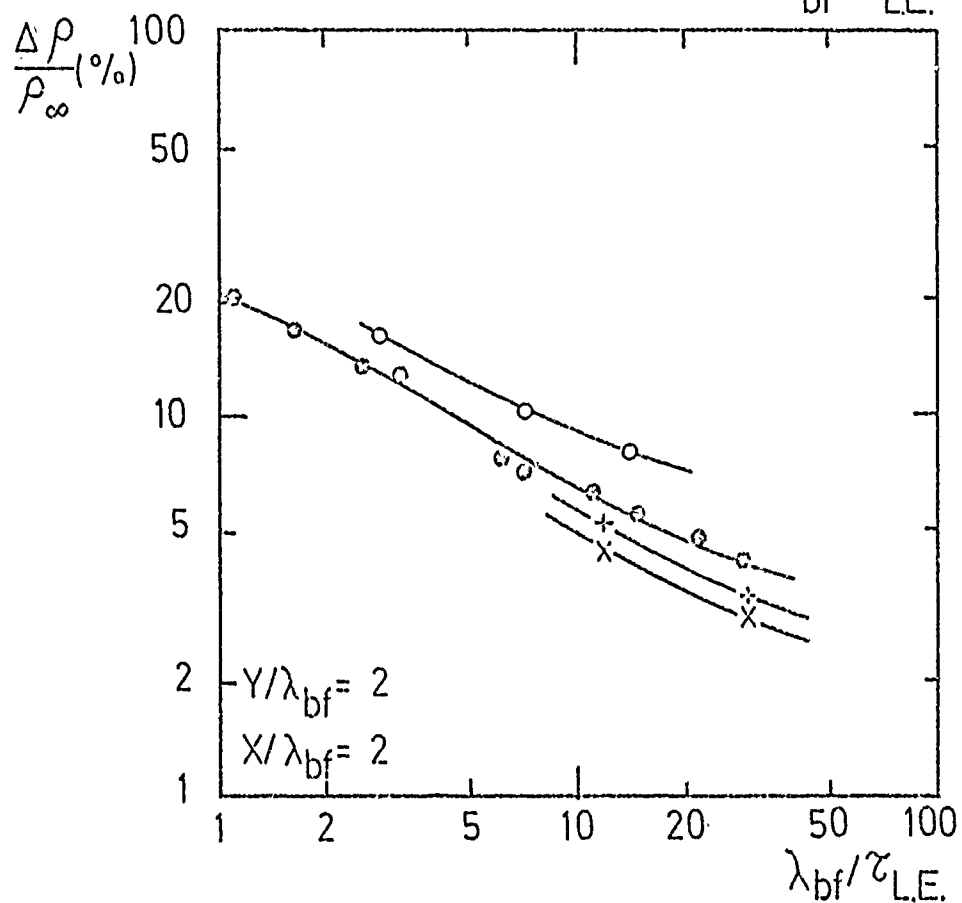
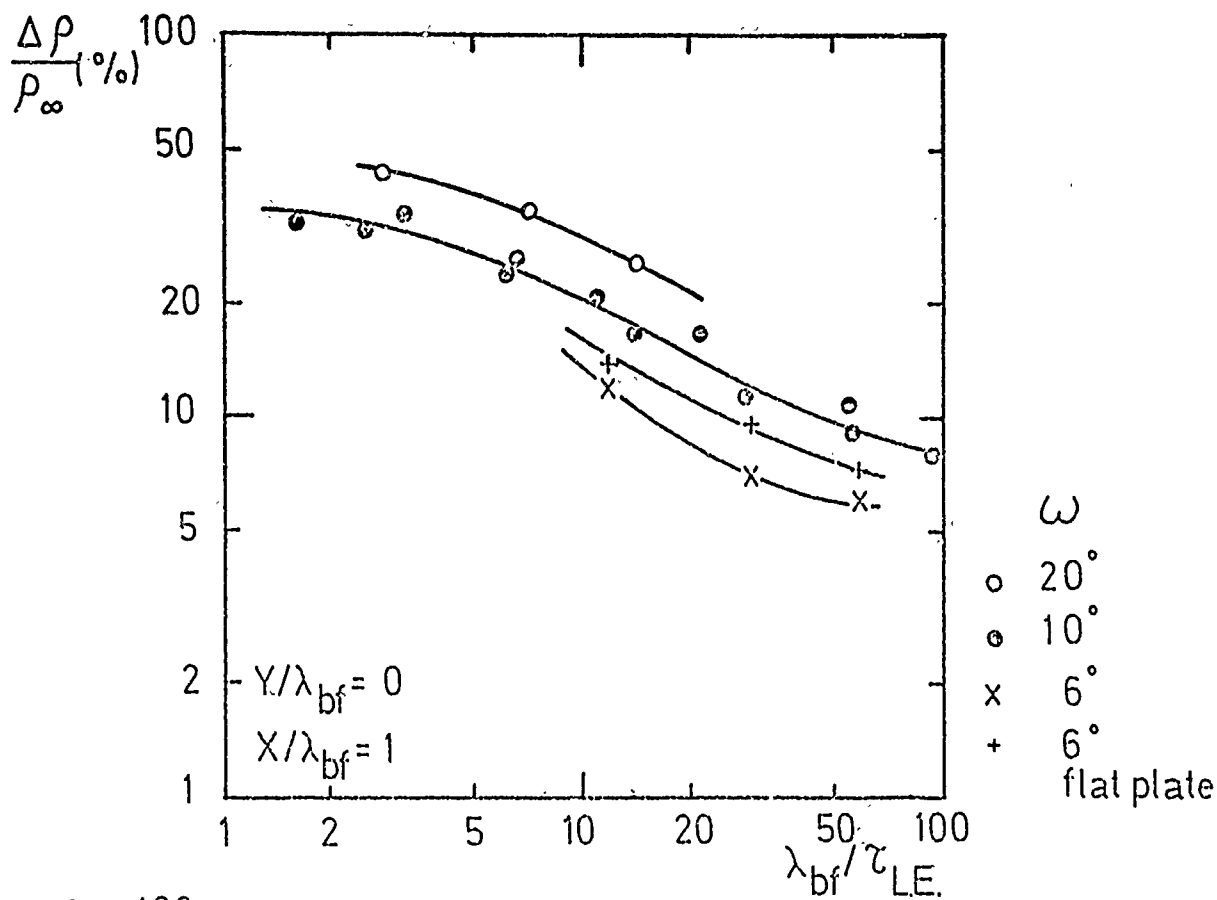
Figure 10



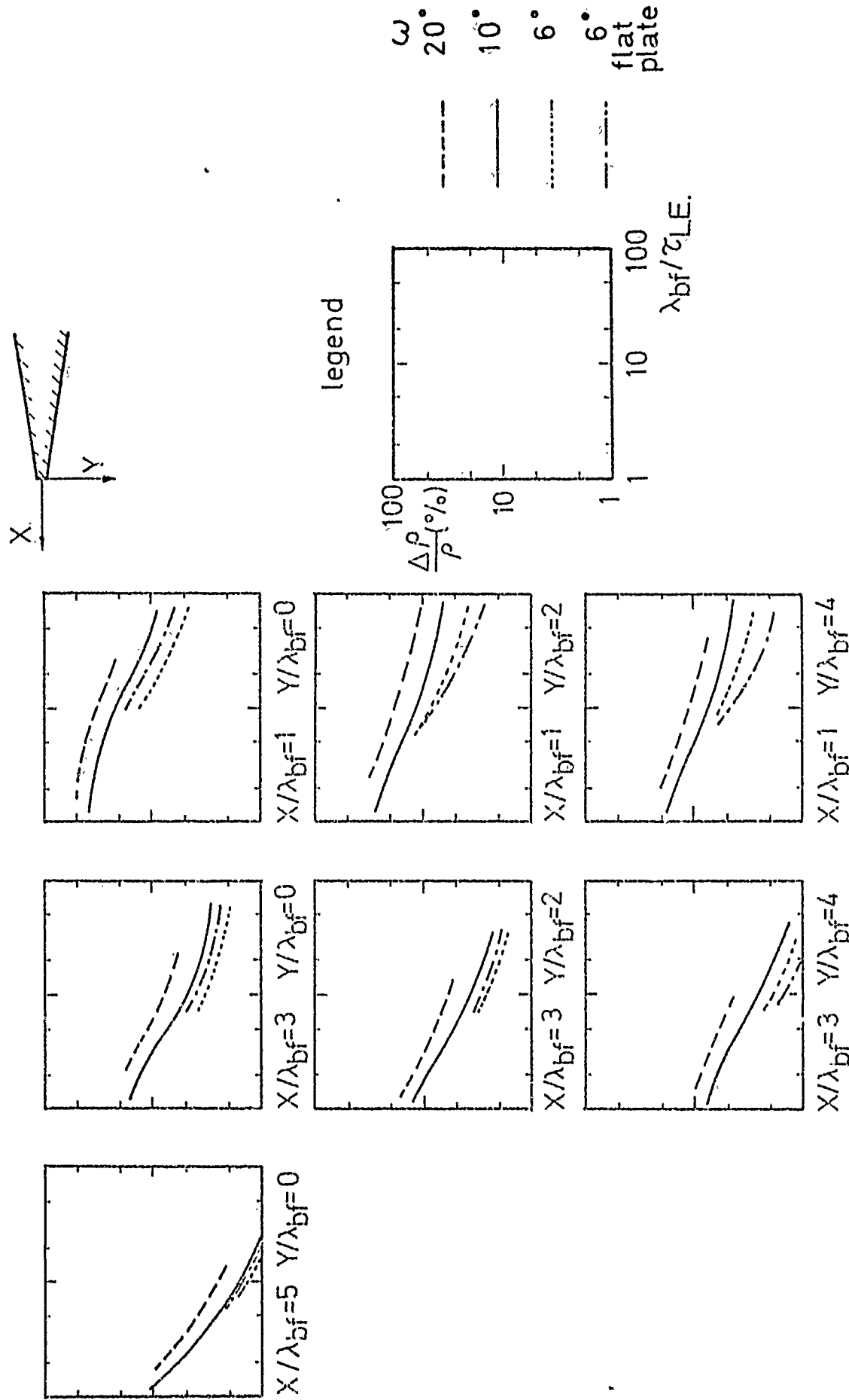
CONSTANT DENSITY PROFILES FOR DIFFERENT GEOMETRICAL CONDITIONS

Figure 11



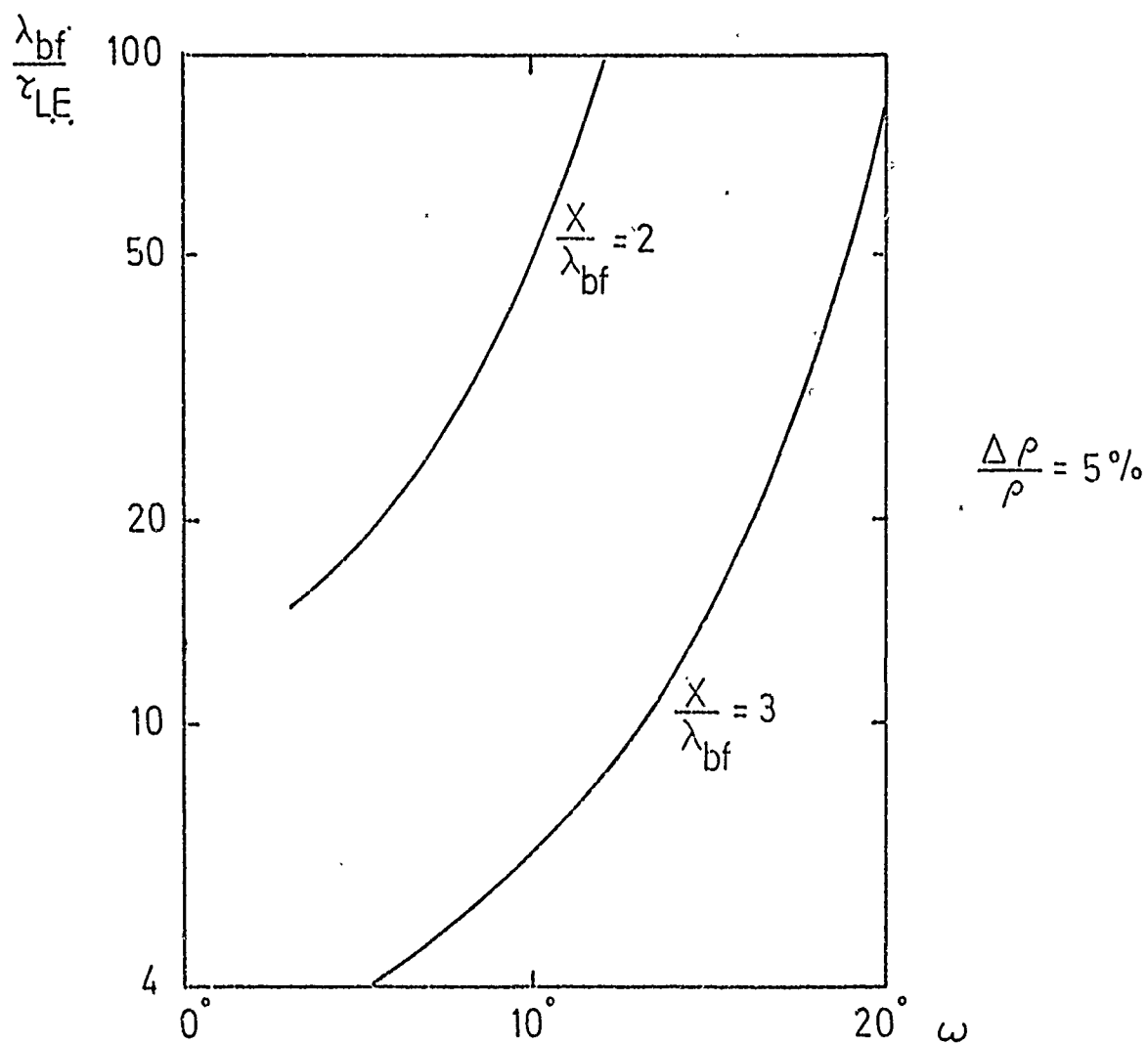


INFLUENCE OF LEADING EDGE THICKNESS ON THE DEVELOPMENT OF THE UPSTREAM DISTURBANCE - TYPICAL RESULTS



INFLUENCE OF LEADING EDGE THICKNESS ON THE DEVELOPMENT OF THE UPSTREAM DISTURBANCE - GENERAL TRENDS

Figure 13



EXTENT OF THE ON-AXIS UPSTREAM DISTURBANCE

Figure 14

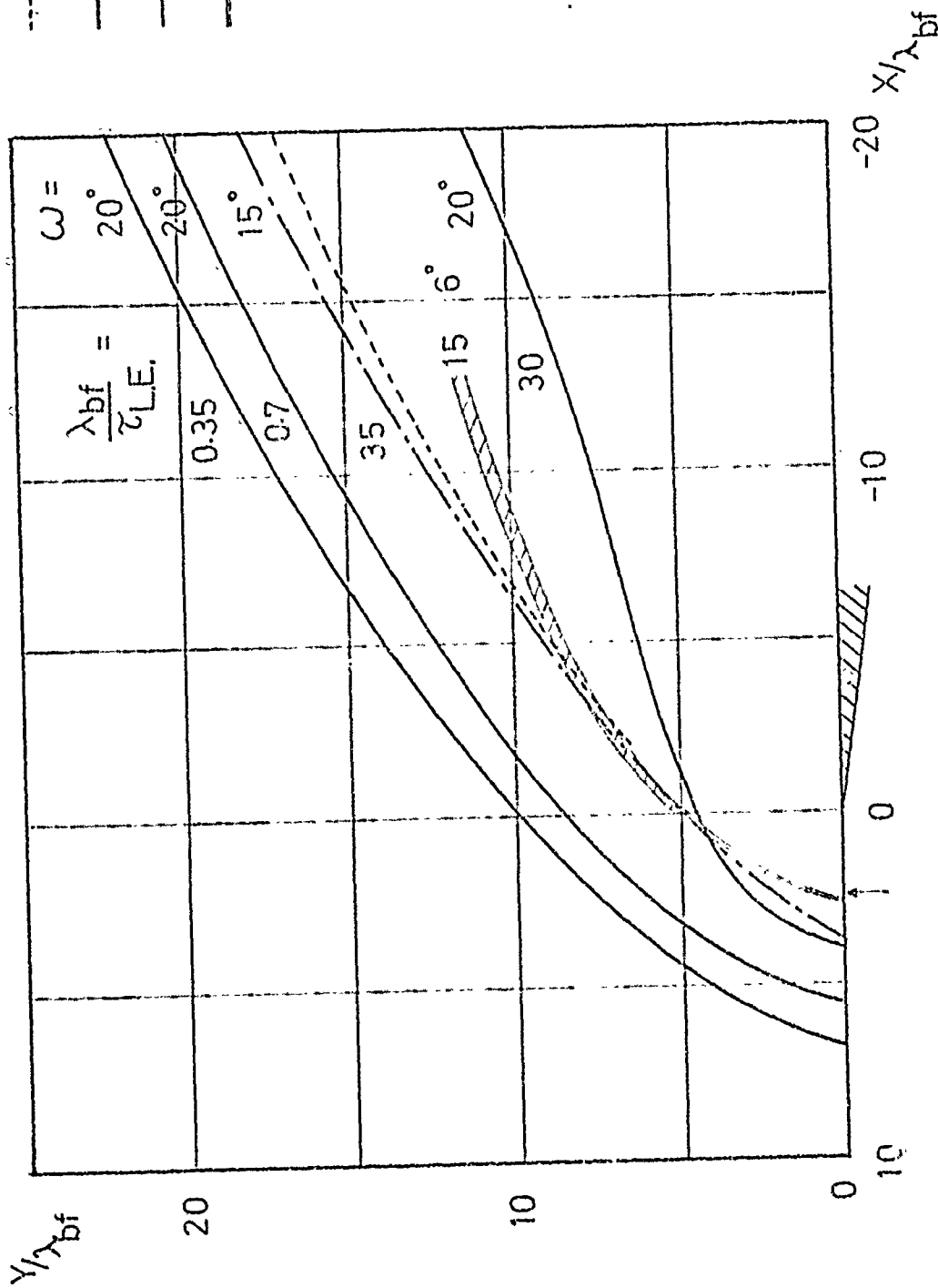
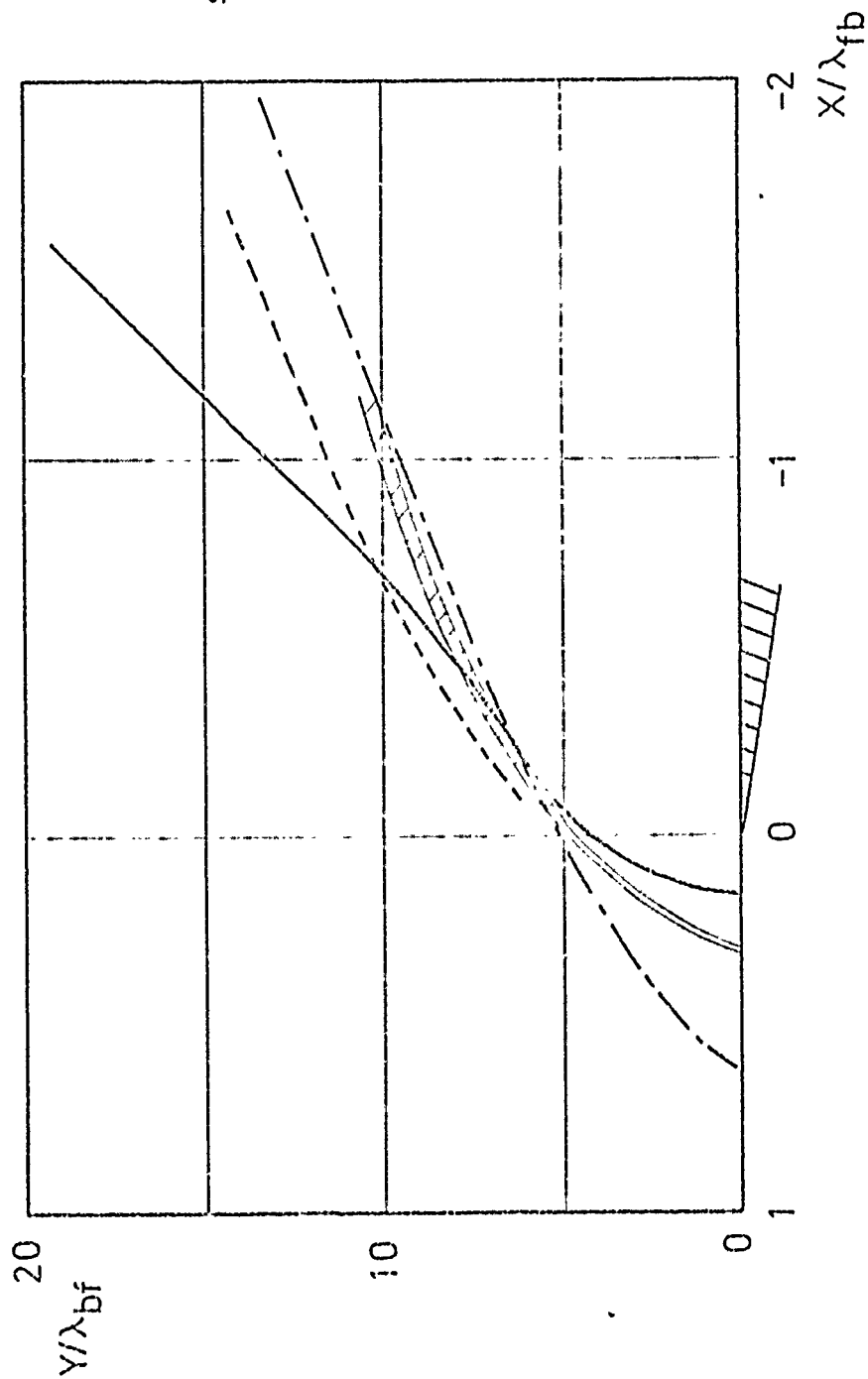


Figure 15

	$M_\infty$	$T_b/T_o$
-----	ref. 7	13
-----	ref. 12	6
-----	ref. 4	26
-----	present	9
↑	ref. 2	9

BOUNDARY OF DENSITY DISTURBANCE FOR FLOW  
OVER A FLAT PLATE - AXIAL DISTANCES NORMALIZED TO  $\lambda_{bf}$



Legend  
same as Fig.15

BOUNDARY OF DENSITY DISTURBANCE FOR FLOW  
OVER A FLAT PLATE - AXIAL DISTANCES NORMALIZED TO  $\lambda_{fb}$

Figure 16

UNCLASSIFIED

Security Classification

## DOCUMENT CONTROL DATA - R &amp; D

(Security classification of title, body of abstract and indexing annotation must be entered when the overall report is classified)

1. ORIGINATING ACTIVITY (Corporate author) VON KARMAN INSTITUTE FOR FLUID DYNAMICS RHODE-SAINT-GENESE, BELGIUM		2a. REPORT SECURITY CLASSIFICATION UNCLASSIFIED	
		2b. GROUP	
3. REPORT TITLE LOW DENSITY HIGH TEMPERATURE GAS DYNAMICS			
4. DESCRIPTIVE NOTES (Type of report and inclusive dates) Scientific Final			
5. AUTHOR(S) (First name, middle initial, last name) J J SMOLDEREN J F WENDT			
6. REPORT DATE 31 Jan 1972		7a. TOTAL NO. OF PAGES 46	7b. NO. OF REFS 26
8a. CONTRACT OR GRANT NO E00AR-70-0081		8b. ORIGINATOR'S REPORT NUMBER(S)	
b. PROJECT NO. 9783-01			
c. 61102F		9b. OTHER REPORT NO(S) (Any other numbers that may be assigned this report)	
d. 681307			
10. DISTRIBUTION STATEMENT Approved for public release; distribution unlimited.			
11. SUPPLEMENTARY NOTES TECH, OTHER		12. SPONSORING MILITARY ACTIVITY AF Office of Scientific Research (NAM) 1400 Wilson Boulevard Arlington, Virginia 22209	
13. ABSTRACT An experimental study was performed to determine the nature of the disturbance to the free stream density in the vicinity of the leading edge of a wedge. The experiments were performed in a free jet flow field. The principal conclusions of this study are: (1) The appropriate scaling length for upstream disturbances is $\lambda_{bf}$ , the body-free stream mean-free path. (2) A negligible influence of leading edge bluntness on upstream density requires that the leading edge thickness obey the relationship leading edge thickness = $\tau_{L,E} \ll \lambda_{bf}/S_\infty$ , where $S_\infty$ is the free stream speed ratio. (3) Upstream influence is strongly affected by both $\tau_{L,E}$ and $\omega$ , the wedge total angle. (4) Limiting on-axis values for $\Delta p/p$ corresponding to the infinitely-thin flat plate case ( $\omega \rightarrow 0$ , $\tau_{L,E} \rightarrow 0$ ) have been determined by extrapolation for various values of $x/\lambda_{bf}$ upstream. At $x \approx 1 \lambda_{bf}$ ( $\Delta p/p$ ) flat plate is $\sim 5\%$ . (5) When the disturbance region is scaled by $\lambda_{bf}$ , good agreement with other experiments and with Monte Carlo calculations is obtained.			

**Security Classification**

UNCLASSIFIED

**Security Classification**